The Astrophysical Journal, 746:150 (20pp), 2012 February 20 doi:10.1088/0004-637X/746/2/150

TIDAL DISSIPATION COMPARED TO SEISMIC DISSIPATION: IN SMALL BODIES, EARTHS, AND SUPER-EARTHS

Michael Efroimsky
U.S. Naval Observatory, Washington, DC 20392, USA; michael.efroimsky@usno.navy.mil
Received 2011 May 16; accepted 2011 November 16; published 2012 February 2

ABSTRACT

While the seismic quality factor and phase lag are defined solely by the bulk properties of the mantle, their tidal counterparts are determined by both the bulk properties and the size effect (self-gravitation of a body as a whole). For a qualitative estimate, we model the body with a homogeneous sphere, and express the tidal phase lag through the lag in a sample of material. Although simplistic, our model is sufficient to understand that the lags are not identical. The difference emerges because self-gravitation pulls the tidal bulge down. At low frequencies, this reduces strain and the damping rate, making tidal damping less efficient in larger objects. At higher frequencies, competition between self-gravitation and rheology becomes more complex, though for sufficiently large super-Earths the same rule applies: the larger the planet, the weaker the tidal dissipation in it. Being negligible for small terrestrial planets and moons, the difference between the seismic and tidal lagging (and likewise between the seismic and tidal damping) becomes very considerable for large exoplanets (super-Earths). In those, it is much lower than what one might expect from using a seismic quality factor. The tidal damping rate deviates from the seismic damping rate, especially in the zero-frequency limit, and this difference takes place for bodies of *any* size. So the equal in magnitude but opposite in sign tidal torques, exerted on one another by the primary and the secondary, have their orbital averages going smoothly through zero as the secondary crosses the synchronous orbit. We describe the mantle rheology with the Andrade model, allowing it to lean toward the Maxwell model at the lowest frequencies. To implement this additional flexibility, we reformulate the Andrade model by endowing it with a free parameter ζ which is the ratio of the anelastic timescale to the viscoelastic Maxwell time of the mantle. Some uncertainty in this parameter's frequency dependence does not influence our principal conclusions.

Key words: celestial mechanics – Earth – Moon – planet–star interactions – planets and satellites: dynamical evolution and stability – planets and satellites: general

1. THE GOAL AND THE PLAN

As the research on exoplanetary systems is gaining momentum, more and more accurate theoretical tools of planetary dynamics come into demand. Among those tools are the methods of calculation of tidal evolution of both orbital and rotational motion of planets and their moons. Such calculations involve two kinds of integral parameters of celestial bodies—the Love numbers and the tidal quality factors. The values of these parameters depend upon the rheology of a body, as well as its size, temperature, and the tidal frequency.

It has recently become almost conventional in the literature to assume that the tidal quality factor of super-Earths should be of the order of one hundred to several hundred (Carter et al. 2011; Léger et al. 2009). Although an acceptable estimate for the seismic Q, this range of numbers turns out to fall short, sometimes by orders of magnitude, of the tidal Q of super-Earths.

In this paper, the frequency dependence of tidal damping in a near-spherical homogeneous body is juxtaposed with the frequency dependence of damping in a sample of the material in which the body consists. For brevity, damping in a sample will be termed (somewhat broadly) "seismic damping."

We shall demonstrate that, while the tidal Q of the solid Earth does not deviate much from the solid-Earth seismic Q, the situation with larger telluric bodies is considerably different. The difference stems from the presence of self-gravitation, which suppresses the tidal bulge and thereby acts as extra rigidity—a long-known circumstance often neglected in astronomical studies.[1] Due to self-gravitation ("size effect"), tidal damping in super-Earths is much less efficient than in Earths, and the difference may come to orders of magnitude, as will be demonstrated below. Thus, while the *seismic* Q of a super-Earth may be comparable to the seismic Q of the solid Earth, the *tidal* Q of a super-Earth may exceed this super-Earth's seismic Q greatly. This is the reason why it is inappropriate to approximate super-Earths' tidal quality factors with that of the solid Earth.

We shall show that the difference between the frequency dependence of the tidal Q factor and that of the seismic Q may explain the "improper" frequency dependence of the tidal dissipation rate measured by the lunar laser ranging (LLR) method. We also shall point out that the correct frequency dependence of the tidal dissipation rate, especially at low frequencies, plays an important role in modeling the process of entrapment into spin–orbit resonances. The latter circumstance will be discussed in greater detail in Efroimsky (2012).

The rate of the "seismic damping" (a term that we employ to also denote damping in a sample of the material) is defined, at each frequency, by the material's rheology only, i.e., by the constitutive equation linking the strain and stress at this frequency. The rate of the tidal damping, however, is determined both by the rheology and by the intensity of self-gravitation of the body. At a qualitative

[1] Including the size effect via k_l is common. Unfortunately, it is commonly assumed sufficient. This treatment, however, is inconsistent in that it ignores the inseparable connection between the Love number and the tidal quality factor (or the tidal phase lag). In reality, both the Love number and the sine of the tidal lag should be derived from the rheology and geometry of the celestial body, and cannot be adjusted separately from one another.

Report Documentation Page

Form Approved
OMB No. 0704-0188

1. REPORT DATE	2. REPORT TYPE	3. DATES COVERED
20 FEB 2012		**00-00-2012 to 00-00-2012**

4. TITLE AND SUBTITLE	5a. CONTRACT NUMBER
Tidal Dissipation Compared To Seismic Dissipation: In Small Bodies, Earths, And Super-Earths	5b. GRANT NUMBER
	5c. PROGRAM ELEMENT NUMBER
6. AUTHOR(S)	5d. PROJECT NUMBER
	5e. TASK NUMBER
	5f. WORK UNIT NUMBER
7. PERFORMING ORGANIZATION NAME(S) AND ADDRESS(ES) **U.S. Naval Observatory,Washington,DC,20392**	8. PERFORMING ORGANIZATION REPORT NUMBER
9. SPONSORING/MONITORING AGENCY NAME(S) AND ADDRESS(ES)	10. SPONSOR/MONITOR'S ACRONYM(S)
	11. SPONSOR/MONITOR'S REPORT NUMBER(S)

12. DISTRIBUTION/AVAILABILITY STATEMENT
Approved for public release; distribution unlimited

13. SUPPLEMENTARY NOTES

14. ABSTRACT

While the seismic quality factor and phase lag are defined solely by the bulk properties of the mantle, their tidal counterparts are determined by both the bulk properties and the size effect (self-gravitation of a body as awhole). For a qualitative estimate, we model the body with a homogeneous sphere, and express the tidal phase lag through the lag in a sample of material. Although simplistic, our model is sufficient to understand that the lags are not identical. The difference emerges because self-gravitation pulls the tidal bulge down. At low frequencies, this reduces strain and the damping rate, making tidal damping less efficient in larger objects. At higher frequencies, competition between self-gravitation and rheology becomes more complex, though for sufficiently large super-Earths the same rule applies: the larger the planet, the weaker the tidal dissipation in it. Being negligible for small terrestrial planets and moons, the difference between the seismic and tidal lagging (and likewise between the seismic and tidal damping) becomes very considerable for large exoplanets (super-Earths). In those, it is much lower than what one might expect from using a seismic quality factor. The tidal damping rate deviates from the seismic damping rate, especially in the zero-frequency limit, and this difference takes place for bodies of any size. So the equal in magnitude but opposite in sign tidal torques, exerted on one another by the primary and the secondary, have their orbital averages going smoothly through zero as the secondary crosses the synchronous orbit. We describe the mantle rheology with the Andrade model, allowing it to lean toward the Maxwell model at the lowest frequencies. To implement this additional flexibility, we reformulate the Andrade model by endowing it with a free parameter ζ which is the ratio of the anelastic timescale to the viscoelastic Maxwell time of the mantle. Some uncertainty in this parameter?s frequency dependence does not influence our principal conclusions.

15. SUBJECT TERMS

16. SECURITY CLASSIFICATION OF:			17. LIMITATION OF ABSTRACT	18. NUMBER OF PAGES	19a. NAME OF RESPONSIBLE PERSON
a. REPORT **unclassified**	b. ABSTRACT **unclassified**	c. THIS PAGE **unclassified**	**Same as Report (SAR)**	**21**	

Standard Form 298 (Rev. 8-98)
Prescribed by ANSI Std Z39-18

level, this can be illustrated by the presence of two terms, 1 and $19\mu(\infty)/(2\rho g R)$, in the denominator of the expression for the static Love number k_2 of a homogeneous sphere. Here $\mu(\infty)$ denotes the relaxed shear modulus and g signifies the surface gravity, while ρ and R stand for the mean density and the radius of the body. The first of these terms, 1, is responsible for the size effect (self-gravitation), and the second stands for the bulk properties of the medium. Within the applicability realm of an important theorem called elastic–viscoelastic analogy (also referred to as the correspondence principle), the same expression interconnects the Fourier component $\bar{k}_2(\chi)$ of the time derivative of the Love number with the Fourier component $\bar{\mu}(\chi)$ of the stress-relaxation function at frequency χ. This renders the frequency dependence of the tangent of the tidal lag, which is the negative ratio of the imaginary and real parts of $\bar{k}_2(\chi)$.

This preliminary consideration illustrates the way rheology enters the picture. First, the constitutive equation defines the frequency dependence of the complex compliance, $\bar{J}(\chi)$, and of the complex rigidity $\bar{\mu}(\chi) = 1/\bar{J}(\chi)$. The functional form of this dependence determines the frequency dependence of the complex Love number, $\bar{k}_l(\chi)$. The latter furnishes the frequency dependence of the products $|\bar{k}_l(\chi)| \sin\epsilon_l(\chi)$ which enter the tidal theory.

In Section 2, we briefly recall the standard description of stress–strain relaxation and dissipation in linear media. In Section 3, we describe a rheological model, which has proven to be adequate to the experimental data on the mantle minerals and partial melts. The goal of the subsequent sections will be to build the rheology into the theory of bodily tides, and to compare a tidal response of a near-spherical body to a seismic response rendered by the medium. Finally, several examples will be provided. Among these will be the case of the Moon whose "improper" tidal dissipation frequency dependence finds an explanation as soon as the difference between the seismic and tidal friction is brought to light. In the closing section, we shall compare our results with those obtained by Goldreich (1963).

The meaning of the symbols used in the text is explained in Table 2 located at the end of the paper.

2. FORMALISM

Everywhere in this paper we shall take into consideration only the deviatoric stresses and strains, thus neglecting compressibility.

2.1. Compliance and Rigidity: The Standard Linear Formalism in the Time Domain

The value of strain in a material depends only on the present and past values taken by the stress and not on the current *rate* of change of the stress. Hence the compliance operator $\hat{J}$ mapping the stress $\sigma_{\gamma\nu}$ to the strain $u_{\gamma\nu}$ must be just an integral operator, linear at small deformations:

$$2\,u_{\gamma\nu}(t) = \hat{J}(t)\,\sigma_{\gamma\nu} = \int_{-\infty}^{t} J(t-t')\;\dot{\sigma}_{\gamma\nu}\,(t')\,dt', \tag{1}$$

where $t' < t$, while overdot denotes d/dt'. The kernel $J(t-t')$ is termed the compliance function or the creep-response function.

Integration by parts renders:

$$2\,u_{\gamma\nu}(t) = \hat{J}(t)\sigma_{\gamma\nu} = J(0)\,\sigma_{\gamma\nu}(t) - J(\infty)\,\sigma_{\gamma\nu}(-\infty) + \int_{-\infty}^{t} \dot{J}\,(t-t')\sigma_{\gamma\nu}(t')dt'. \tag{2}$$

As the load in the infinite past may be set zero, the term containing the relaxed compliance $J(\infty)$ may be dropped. The unrelaxed compliance $J(0)$ can be absorbed into the integral if we agree that the elastic contribution enters the compliance function not as

$$J(t-t') = J(0) + \text{viscous and hereditary terms}, \tag{3}$$

but as

$$J(t-t') \;=\; J(0)\,\Theta(t-t') \;+\; \text{viscous and hereditary terms}. \tag{4}$$

The Heaviside step-function $\Theta(t-t')$ is set unity for $t - t' \geqslant 0$, and zero for $t - t' < 0$, so its derivative is the delta-function $\delta(t-t')$. Keeping this in mind, we reshape Equation (2) into

$$2\,u_{\gamma\nu}(t) = \hat{J}(t)\sigma_{\gamma\nu} = \int_{-\infty}^{t} \dot{J}\,(t-t')\sigma_{\gamma\nu}(t')\,dt', \quad \text{with } J(t-t') \text{ containing } J(0)\,\Theta(t-t'). \tag{5}$$

Inverse to the compliance operator

$$2\,u_{\gamma\nu} = \hat{J}\sigma_{\gamma\nu} \tag{6}$$

is the rigidity operator

$$\sigma_{\gamma\nu} = 2\,\hat{\mu}u_{\gamma\nu}. \tag{7}$$

In the presence of viscosity, the operator $\hat{\mu}$ is not integral but is integrodifferential, and thus cannot be expressed as $\sigma_{\gamma\nu}(t) = 2\int_{-\infty}^{t} \dot{\mu}(t-t')\,u_{\gamma\nu}(t')\,dt'$. It can, though, be written as

$$\sigma_{\gamma\nu}(t) = 2\int_{-\infty}^{t} \mu(t-t')\,\dot{u}_{\gamma\nu}(t')\,dt', \tag{8}$$

if its kernel, the stress-relaxation function $\mu(t-t')$, is imparted with a term $2\,\eta\,\delta(t-t')$, integration whereof renders the viscous portion of stress, $2\,\eta\,\dot{u}_{\gamma\nu}$. The kernel also incorporates an unrelaxed part $\mu(0)\,\Theta(t-t')$ whose integration furnishes the elastic portion of the stress. The unrelaxed rigidity $\mu(0)$ is inverse to the unrelaxed compliance $J(0)$.

Each term in $\mu(t-t')$, which is neither constant nor proportional to a delta function, is responsible for hereditary reaction.

2.2. In the Frequency Domain

To Fourier-expand a real function, nonnegative frequencies are sufficient. Thus, we write

$$\sigma_{\gamma\nu}(t)=\int_0^\infty \bar{\sigma}_{\gamma\nu}(\chi)e^{i\chi t}d\chi \quad \text{and} \quad u_{\gamma\nu}(t)=\int_0^\infty \bar{u}_{\gamma\nu}(\chi)e^{i\chi t}d\chi\,, \tag{9}$$

where the complex amplitudes are

$$\bar{\sigma}_{\gamma\nu}(\chi)=\sigma_{\gamma\nu}(\chi)e^{i\varphi_\sigma(\chi)}, \quad \bar{u}_{\gamma\nu}(\chi)=u_{\gamma\nu}(\chi)e^{i\varphi_u(\chi)}, \tag{10}$$

while the initial phases $\varphi_\sigma(\chi)$ and $\varphi_u(\chi)$ are set to render the real amplitudes $\sigma_{\gamma\nu}(\chi_n)$ and $u_{\gamma\nu}(\chi_n)$ nonnegative. To ensure convergence, the frequency is, whenever necessary, assumed to approach the real axis from below: $\mathcal{I}m(\chi)\to 0-$.

With the same caveats, the complex compliance $\bar{J}(\chi)$ is introduced as the Fourier image of the time derivative of the creep-response function:

$$\int_0^\infty \bar{J}(\chi)\,e^{i\chi\tau}d\chi=\dot{J}\,(\tau). \tag{11}$$

The inverse expression,

$$\bar{J}(\chi)=\int_0^\infty \dot{J}\,(\tau)\,e^{-i\chi\tau}\,d\tau, \tag{12}$$

is often written as

$$\bar{J}(\chi)=J(0)+i\,\chi\int_0^\infty [J(\tau)-J(0)\,\Theta(\tau)]\,e^{-i\chi\tau}\,d\tau. \tag{13}$$

For causality reasons, the integration over τ spans the interval $[0,\infty]$ only. Alternatively, we can accept the convention that *each* term in the creep-response function is accompanied by the Heaviside step function.

Insertion of the Fourier integrals (9)–(11) into Equation (1) leads us to

$$2\int_0^\infty \bar{u}_{\gamma\nu}(\chi)e^{i\chi t}d\chi=\int_0^\infty \bar{\sigma}_{\mu\nu}(\chi)\bar{J}(\chi)e^{i\chi t}d\chi\,, \tag{14}$$

whence we obtain

$$2\,\bar{u}_{\gamma\nu}(\chi)=\bar{J}(\chi)\,\bar{\sigma}_{\gamma\nu}(\chi). \tag{15}$$

Expressing the complex compliance as

$$\bar{J}(\chi)=|\bar{J}(\chi)|\exp[-i\,\delta(\chi)\,], \tag{16}$$

where

$$\tan\delta(\chi)\equiv-\frac{\mathcal{I}m[\,\bar{J}(\chi)\,]}{\mathcal{R}e[\,\bar{J}(\chi)\,]}, \tag{17}$$

we see that $\delta(\chi)$ is the phase lag of a strain harmonic mode relative to the appropriate harmonic mode of the stress:

$$\varphi_u(\chi)=\varphi_\sigma(\chi)-\delta(\chi). \tag{18}$$

2.3. The Quality Factor(s)

In the linear approximation, at each frequency χ the average (per period) energy dissipation rate $\langle\dot{E}\,(\chi)\rangle$ is defined by the deformation at that frequency only, and bears no dependence upon the other frequencies:

$$\langle\dot{E}(\chi)\rangle=-\frac{\chi\,E_{\rm peak}(\chi)}{Q(\chi)} \tag{19}$$

or, the same:

$$\Delta E_{\rm cycle}(\chi) = -\frac{2\pi\, E_{\rm peak}(\chi)}{Q(\chi)}, \tag{20}$$

$\Delta E_{\rm cycle}(\chi)$ being the one-cycle energy loss and $Q(\chi)$ being the quality factor related to the phase lag at the frequency χ. It should be clarified right away to which of the lags we are linking the quality factor. When we are talking about a sample of material, this lag is simply $\delta(\chi)$ introduced above as the negative argument of the appropriate Fourier component of the complex compliance—see formulae (17) and (18). However, whenever we address tide, the quality factor becomes linked (via the same formulae) to the *tidal* phase lag $\epsilon(\chi)$. Within the same rheological model, the expression for $\epsilon(\chi)$ differs from that for $\delta(\chi)$, because the tidal lag depends not only upon the local properties of the material, but also upon self-gravitation of the body as a whole.

The aforementioned "seismic-or-tidal" ambiguity in the definition of Q becomes curable as soon as one points out to which kind of deformation the quality factor pertains. More serious is the ambiguity stemming from the freedom in defining $E_{\rm peak}(\chi)$.

If $E_{\rm peak}(\chi)$ in Equations (19) and (20) signifies the peak *energy* stored at frequency χ, the resulting quality factor is related to the lag via

$$Q^{-1}_{\rm energy} = \sin|\delta| \tag{21}$$

(not $\tan|\delta|$ as commonly believed—see the calculation in the Appendix to Efroimsky 2012).

If, however, $E_{\rm peak}(\chi)$ is introduced as the absolute maximum of *work* carried out on the sample at frequency χ over a time interval through which the power stays positive, then the appropriate Q factor is connected to the lag via

$$Q^{-1}_{\rm work} = \frac{\tan|\delta|}{1-((\pi/2)-|\delta|)\tan|\delta|}, \tag{22}$$

as was shown in Efroimsky (2012).[2]

The third definition of the quality factor (offered by Goldreich 1963) is

$$Q^{-1}_{\rm Goldreich} = \tan|\delta|. \tag{23}$$

This definition, though, corresponds neither to the peak work nor to the peak energy.

In the limit of weak lagging, all three definitions entail

$$Q^{-1} = |\delta| + O(\delta^2). \tag{24}$$

For the lag approaching $\pi/2$, the quality factor defined as (21) assumes its minimal value, $Q_{\rm energy} = 1$, while definition (22) renders $Q_{\rm work} = 0$. The latter is natural, since in the considered limit the work performed on the system is negative, its absolute peak being zero.[3]

In seismic studies or in exploration of attenuation in small samples, one's choice among the three definitions of Q is a matter of personal taste, for the quality factor is large and the definitions virtually coincide.

In the theory of tides, the situation is different, because at times one has to deal with situations where the definitions of Q disagree noticeably—this happens when dissipation is intensive and Q is of order unity. To make a choice, recall that the actual quantities entering the Fourier expansion of tides over the modes ω_{lmpq} are the products[4]

$$k_l\ \sin\epsilon_l = k_l(\omega_{lmpq})\sin\epsilon_l(\omega_{lmpq}), \tag{25}$$

where $k_l(\omega_{lmpq})$ are the dynamical analogs to the Love numbers. It is these products that show up in the $lmpq$ terms of the expansion for the tidal potential (force, torque). From this point of view, a definition like Equation (21) would be preferable, though this time with the tidal lag ϵ instead of the seismic lag δ:

$$Q_l^{-1} = \sin|\epsilon_l| \tag{26a}$$

or, in a more detailed manner:

$$Q_l^{-1}(\omega_{lmpq}) = \sin|\epsilon_l(\omega_{lmpq})|. \tag{26b}$$

Under this definition, one is free to substitute $k_l\ \sin\epsilon_l$ with k_l/Q_l. The subscript l accompanying the tidal quality factor will then serve as a reminder of the distinction between the tidal quality factor and its seismic counterpart.

While the notion of the tidal quality factor has some illustrative power and may be employed for rough estimates, calculations involving bodily tides should be based not on the knowledge of the quality factor but on the knowledge of the overall frequency dependence of products $k_l\ \sin\epsilon_l = k_l(\omega_{lmpq})\ \sin\epsilon_l(\omega_{lmpq})$. Relying on these functions would spare one the ambiguity in the definition of Q and would also enable one to take into account the frequency dependence of the dynamical Love numbers.

---

[2] In Efroimsky & Williams (2009), $E_{\rm peak}(\chi)$ was misnamed "peak energy." However, the calculation of Q was performed there for $E_{\rm peak}(\chi)$ introduced as the peak *work*.

[3] As $Q < 2\pi$ implies $E_{\rm peak} < \Delta E$, such small values of Q are unattainable in the case of damped free oscillations. Still, Q can assume such values under excitation, tides being the case.

[4] A historical tradition (originating from Kaula 1964) prescribes to denote the tidal phase lags with ϵ_{lmpq}, while keeping for the dynamical Love numbers the same notation as for their static predecessors: k_l. These conventions are in conflict because the product $k_l\ \sin\epsilon_{lmpq}$ is the negative imaginary part of the complex Love number $\bar{k}_l$. More logical is to use the unified notation as in Equation (25). At the same time, it should not be forgotten that for triaxial bodies the functional form of the dependence of $\bar{k}_l$ on frequency is defined not only by l but also by $m,\ p,\ q$. In those situations, one has to deal with $k_{lmpq}\ \sin\epsilon_{lmpq}$, see Section 4.

3. THE ANDRADE MODEL AND ITS REPARAMETERIZATION

In the low-frequency limit, the mantle's behavior is unlikely to differ much from that of the Maxwell body because over timescales much longer than 1 yr viscosity dominates (Karato & Spetzler 1990). At the same time, the accumulated geophysical, seismological, and geodetic observations suggest that at shorter timescales anelasticity takes over and the mantle is described by the Andrade model. However, the near-Maxwell behavior expected at low frequencies can be fit into the Andrade formalism, as we shall explain below.

3.1. Experimental Data: The Power Scaling Law

Dissipation in solids may be effectively modeled using the empirical scaling law

$$\sin\delta = (\mathcal{E}\,\chi)^{-p}, \tag{27}$$

$\mathcal{E}$ being a constant having the dimensions of time. This "constant" may itself bear a (typically, much slower) dependence upon the frequency χ. The dependence of $\mathcal{E}$ on the temperature is given by the Arrhenius law (Karato 2008).

Experiments demonstrate that the power dependence (27) is surprisingly universal, with the exponential p robustly taking values within the interval from 0.14 to 0.4 (more often, from 0.14 to 0.3).

For the first time, dependence (27) was measured on metals in a lab. This was done by Andrade (1910), who also tried to pick up an expression for the compliance compatible with this scaling law. Later studies have demonstrated that this law works equally well, and with similar values of p, both for silicate rocks (Weertman & Weertman 1975; Tan et al. 1997) and ices (Castillo-Rogez et al. 2009; McCarthy et al. 2007).

Independent from the studies of samples in the lab, the scaling behavior (Equation (27)) was obtained via measurements of dissipation of seismic waves in the Earth (Mitchell 1995; Stachnik et al. 2004; Shito et al. 2004).

The third source of confirmation of the power scaling law came from geodetic experiments that included: (1) satellite laser ranging (SLR) of tidal variations in the J_2 component of the gravity field of the Earth, (2) space-based observations of tidal variations in Earth's rotation rate, and (3) space-based measurements of the Chandler wobble period and damping (Benjamin et al. 2006; Eanes & Bettadpur 1996; Eanes 1995).[5]

While samples of most minerals furnish values of p lying within the interval 0.15–0.4, the geodetic measurements give 0.14–0.2. At least a fraction of this difference may be attributed to the presence of partial melt, which is known to have lower values of p (Fontaine et al. 2005).

On all of these grounds, it is believed that mantles of terrestrial planets are adequately described by the Andrade model, at least in the higher-frequency band where anelasticity dominates (Gribb & Cooper 1998; Birger 2007; Efroimsky & Lainey 2007; Zharkov & Gudkova 2009). Some of the other models were considered by Henning et al. (2009).

The Andrade model is equally well applicable to celestial bodies with ice mantles (for application to Iapetus see Castillo-Rogez et al. 2011) and to bodies with considerable hydration in a silicate mantle.[6] The model can also be employed for modeling of the tidal response *of the solid parts* of objects with significant liquid-water layers.[7]

3.2. The Andrade Model in the Time Domain

The compliance function of the Andrade body (Cottrell & Aytekin 1947; Duval 1978),

$$J(t-t') = [J + (t-t')^{\alpha}\beta + (t-t')\eta^{-1}]\,\Theta(t-t'), \tag{28}$$

contains empirical parameters α and β, the steady-state viscosity η, and the unrelaxed compliance $J \equiv J(0) = 1/\mu(0) = 1/\mu$. We endow the right-hand side of Equation (28) with the Heaviside step-function $\Theta(t-t')$ to ensure that insertion of Equation (28) into Equation (5), with the subsequent differentiation, yields the elastic term $J\,\delta(t-t')$ under the integral. The model allows for description of dissipation mechanisms over a continuum of frequencies, which is useful for complex materials with a range of grain sizes.

The Andrade model can be thought of as the Maxwell model equipped with an extra term $(t-t')^{\alpha}\,\beta$ describing hereditary reaction of strain to stress. The Maxwell model

$$J^{(\mathrm{Maxwell})}(t-t') = [J + (t-t')\eta^{-1}]\,\Theta(t-t') \tag{29}$$

is a simple rheology, which has a long history of application to planetary problems, but generally has too strong a frequency dependence at higher frequencies where anelasticity becomes more efficient than viscosity (Karato 2008). Insertion of Equation (29) into Equation (5) renders strain consisting of two separate inputs. The one proportional to J implements the instantaneous (elastic) reaction, while the one containing η^{-1} is responsible for the viscous part of the reaction.

Just as the viscous term $(t-t')\,\eta^{-1}$ showing up in Equations (28) and (29) is delayed, so is the anelastic term $(t-t')^{\alpha}\,\beta$ emerging in the Andrade model (28)—both terms reflect how the past stressing is influencing the present deformation. At the same time, the anelastic reaction differs from viscosity both mathematically and physically because it is produced by different physical mechanisms.

[5] It should be noted that in reality the geodetic measurements were confirming the power law (27) not for the seismic lag δ but for the tidal lag ϵ, an important detail to be addressed shortly.

[6] Damping mechanisms in a wet planet will be the same as in a dry one, except that their efficiency will be increased. Hence, the dissipation rate will have a similar frequency dependence but higher magnitude.

[7] In the absence of internal oceans, a rough estimate of the tidal response can be obtained through modeling the body with a homogeneous sphere. However, the presence of such oceans makes it absolutely necessary to calculate the overall response through integration over the solid and liquid layers. As demonstrated by Tyler (2009), tidal dissipation in internal ocean layers can play a big role in rotational dynamics of the body.

A disadvantage of the formulation (28) of the Andrade model is that it contains a parameter of fractional dimensions, β. To avoid fractional dimensions, we shall express this parameter, following Efroimsky (2012), as

$$\beta = J\,\tau_A^{-\alpha} = \mu^{-1}\,\tau_A^{-\alpha}, \tag{30a}$$

the new parameter τ_A having dimensions of time. This is the timescale associated with the Andrade creep, wherefore it may be named as the "Andrade time" or the "anelastic time."

Another option is to express β as

$$\beta = \zeta^{-\alpha}\,J\,\tau_M^{-\alpha} = \zeta^{-\alpha}\,\mu^{-1}\,\tau_M^{-\alpha}, \tag{30b}$$

where the dimensionless parameter ζ is related through

$$\zeta = \frac{\tau_A}{\tau_M} \tag{31}$$

to the anelastic timescale τ_A and to the Maxwell time

$$\tau_M \equiv \frac{\eta}{\mu} = \eta\,J. \tag{32}$$

In terms of the so-introduced parameters, the compliance assumes the form of

$$J(t-t') = J\left[\,1+\left(\frac{t-t'}{\tau_A}\right)^{\alpha}+\frac{t-t'}{\tau_M}\,\right]\Theta(t-t') \tag{33a}$$

$$= J\left[\,1+\left(\frac{t-t'}{\zeta\,\tau_M}\right)^{\alpha}+\frac{t-t'}{\tau_M}\,\right]\Theta(t-t'). \tag{33b}$$

For $\tau_A \ll \tau_M$ (or, equivalently, for $\zeta \ll 1$), anelasticity plays a more important role than viscosity. On the other hand, a large τ_A (or large ζ) would imply suppression of anelasticity, compared to viscosity.

It has been demonstrated by Castillo-Rogez that under low stressing (i.e., when the grain-boundary diffusion is the dominant damping mechanism—like in Iapetus) β obeys the relation

$$\beta \approx J\,\tau_M^{-\alpha} = J^{1-\alpha}\,\eta^{-\alpha} = \mu^{\alpha-1}\,\eta^{-\alpha} \tag{34a}$$

(see, e.g., Castillo-Rogez et al. 2011). Comparing this to Equation (30), we can say that the anelastic and viscoelastic timescales are close to one another:

$$\tau_A \approx \tau_M \tag{34b}$$

or, equivalently, that the dimensionless parameter ζ is close to unity:

$$\zeta \approx 1. \tag{34c}$$

Generally, we have no reason to expect the anelastic and viscoelastic timescales to coincide, or even to be comparable under all possible circumstances. While Equation (34) may work when the grain-boundary diffusion dominates anelastic friction, we are also aware of a case when the timescales τ_A and τ_M differ considerably. This is a situation when stressing is stronger, and the anelastic part of dissipation is dominated by dislocations unpinning. This is what happens in mantles of Earths and super-Earths.

On theoretical grounds, Karato & Spetzler (1990) point out that the dislocation–unpinning mechanism remains effective in Earth's mantle down to the frequency threshold $\chi_0 \sim 1\mathrm{yr}^{-1}$. At lower frequencies, this mechanism becomes less efficient, giving way to viscosity. Thus, at low frequencies, the mantle's behavior becomes closer to that of the Maxwell body.[8] This important example tells us that the anelastic time τ_A and the dimensionless parameter ζ may, at times, be more sensitive to the frequency than the Maxwell time would be. Whether τ_A and ζ demonstrate this sensitivity or not may, in its turn, depend upon the intensity of loading, i.e., upon the damping mechanisms involved.

3.3. The Andrade Model in the Frequency Domain

Through Equation (12), it can be demonstrated (Findley et al. 1976) that in the frequency domain the compliance of an Andrade material reads as

$$\bar{J}\,(\chi) = J + \beta\,(i\,\chi)^{-\alpha}\,\Gamma\,(1+\alpha) - \frac{i}{\eta\chi} \tag{35a}$$

[8] Using the Andrade model as a fit to the experimentally observed scaling law (27), we see that the exponential p coincides with the Andrade parameter $\alpha < 1$ at frequencies above the said threshold, and that p becomes closer to unity below the threshold—see Section 3.4 below.

$$= J\,[1+(i\,\chi\,\tau_A)^{-\alpha}\,\Gamma(1+\alpha)-i(\chi\,\tau_M)^{-1}], \tag{35b}$$

$$= J\,[1+(i\,\chi\,\zeta\,\tau_M)^{-\alpha}\,\Gamma(1+\alpha)-i(\chi\,\tau_M)^{-1}], \tag{35c}$$

χ being the frequency and Γ denoting the gamma function. The imaginary and real parts of the complex compliance are

$$\mathcal{I}m[\bar{J}(\chi)] = -\frac{1}{\eta\,\chi} - \chi^{-\alpha}\,\beta\,\sin\left(\frac{\alpha\,\pi}{2}\right)\,\Gamma(\alpha+1) \tag{36a}$$

$$= -J\,(\chi\,\tau_M)^{-1} - J\,(\chi\,\tau_A)^{-\alpha}\,\sin\left(\frac{\alpha\,\pi}{2}\right)\,\Gamma(\alpha+1) \tag{36b}$$

$$= -J\,(\chi\,\tau_M)^{-1} - J\,(\chi\,\zeta\,\tau_M)^{-\alpha}\,\sin\left(\frac{\alpha\,\pi}{2}\right)\,\Gamma(\alpha+1) \tag{36c}$$

and

$$\mathcal{R}e[\bar{J}(\chi)] = J + \chi^{-\alpha}\,\beta\,\cos\left(\frac{\alpha\,\pi}{2}\right)\,\Gamma(\alpha+1) \tag{37a}$$

$$= J + J\,(\chi\,\tau_A)^{-\alpha}\,\cos\left(\frac{\alpha\,\pi}{2}\right)\,\Gamma(\alpha+1) \tag{37b}$$

$$= J + J\,(\chi\,\zeta\,\tau_M)^{-\alpha}\,\cos\left(\frac{\alpha\,\pi}{2}\right)\,\Gamma(\alpha+1). \tag{37c}$$

The ensuing frequency dependence of the phase lag will be[9]

$$\tan\delta(\chi) = -\frac{\mathcal{I}m[\bar{J}(\chi)]}{\mathcal{R}e[\bar{J}(\chi)]} = \frac{(\eta\,\chi)^{-1}+\chi^{-\alpha}\,\beta\,\sin[(\alpha\pi)/2]\,\Gamma(\alpha+1)}{\mu^{-1}+\chi^{-\alpha}\,\beta\,\cos[(\alpha\pi)/2]\,\Gamma(\alpha+1)} \tag{38a}$$

$$= \frac{[(1/\chi\tau_M)+(1/\chi\tau_A)^{\alpha}]\,[\Gamma(\alpha+1)\,\sin(\alpha\pi/2)]}{[1+(1/\chi\tau_A)^{\alpha}]\,[\Gamma(\alpha+1)\,\cos(\alpha\pi/2)]} = \frac{z^{-1}\,\zeta+z^{-\alpha}\,\sin(\alpha\pi/2)\,\Gamma(\alpha+1)}{1+z^{-\alpha}\,\cos(\alpha\pi/2)\,\Gamma(\alpha+1)}, \tag{38b}$$

with z being the dimensionless frequency defined through

$$z \equiv \chi\,\tau_A = \chi\,\tau_M\,\zeta. \tag{39}$$

Evidently, for $\beta \to 0$ (that is, for $\zeta \to \infty$ or $\tau_A \to \infty$), expression (38) approaches

$$\tan\delta(\chi) = (\tau_M\,\chi)^{-1}, \tag{40}$$

which is the frequency dependence appropriate to the Maxwell body.

3.4. Low Frequencies: From Andrade toward Maxwell

The Andrade body demonstrates the so-called elbow dependence of the dissipation rate upon frequency. At high frequencies, the lag δ satisfies the power law

$$\tan\delta \sim \chi^{-p}, \tag{41}$$

the exponential being expressed via an empirical parameter α, where $0 < \alpha < 1$ for most materials. It follows from Equation (38) that at higher frequencies $p = \alpha$, while at low frequencies $p = 1-\alpha$.

The statement by Karato & Spetzler (1990), that the mantle's behavior at low frequencies should lean toward that of the Maxwell body, can be fit into the Andrade formalism if we agree that at low frequencies either α approaches zero (so p approaches unity) or ζ becomes large (so τ_A becomes much larger than τ_M). The latter option is more physical because the increase of τ_A would reflect the slowing down of the unpinning mechanism studied in Karato & Spetzler (1990).

One way or another, the so-parameterized Andrade model is fit to embrace the result from Karato & Spetzler (1990). Hence, our treatment will permit us to describe both the high-frequency range where the traditional Andrade model is applicable, and the low-frequency band where the behavior of the mantle deviates from the Andrade model toward the Maxwell body. Comparison of the two models in the frequency domain is presented in Figure 1.

[9] In some publications (e.g., Nimmo 2008), formula (38a) is given as an expression for the inverse quality factor. This is legitimate when the latter is defined through Equation (23).

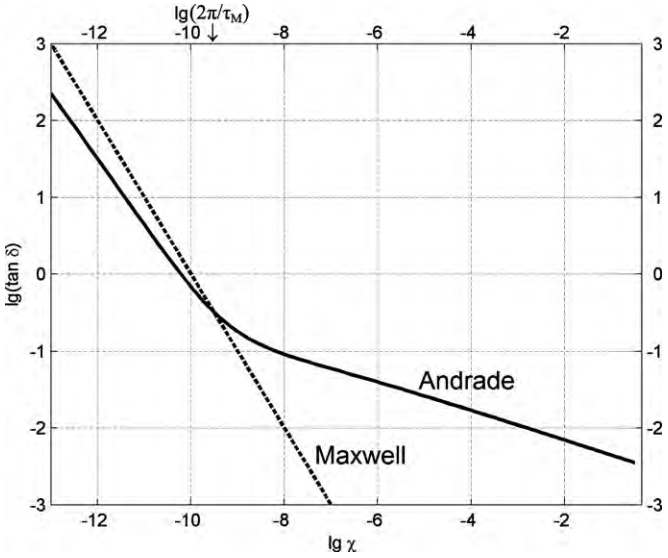

Figure 1. Andrade and Maxwell models in the frequency domain. The plot shows the decadic logarithm of $\tan\delta$, as a function of the decadic logarithm of the forcing frequency χ (in cycles s^{-1}). For the Andrade body, the tangent of phase lag is given by Equation (38b), with $\alpha = 0.2$ and $\tau_A = \tau_M = 10^{10}$ s. For the Maxwell body, the tangent is rendered by Equation (40), with $\tau_M = 10^{10}$ s.

4. EXPANDING A TIDAL POTENTIAL OR TORQUE—OVER THE TIDAL MODES OR OVER THE FORCING FREQUENCIES?

Consider a binary system with mean motion n, and suppose that tidal dissipation in one of the bodies much exceeds that in its companion. Then the former body may be treated as the tidally perturbed primary, the latter being its tide-raising secondary. The sidereal angle and the spin rate of the primary will be expressed with θ and $\dot{\theta}$, while the node, pericenter, and mean anomaly of the secondary, as seen from the primary,[10] will be denoted by Ω, ω, and $\mathcal{M}$.

In the Darwin–Kaula theory, bodily tides are expanded over the modes

$$\omega_{lmpq} \equiv (l-2p)\,\dot{\omega} + (l-2p+q)\,\dot{\mathcal{M}} + m\,(\dot{\Omega}-\dot{\theta}) \approx (l-2p+q)\,n - m\,\dot{\theta}, \tag{42}$$

with $l,\ m,\ p,\ q$ being integers. Dependent upon the values of the mean motion, spin rate, and the indices, the tidal modes ω_{lmpq} may be positive or negative or zero.

In the expansion of the tidal potential or torque or force, summation over the integer indices goes as $\sum_{l=2}^{\infty}\sum_{m=0}^{l}\sum_{p=0}^{\infty}\sum_{q=-\infty}^{\infty}\cdot$. For example, the secular polar component of the tidal torque will read as

$$\mathcal{T} = \sum_{l=2}^{\infty}\sum_{m=0}^{l}\sum_{p=0}^{\infty}\sum_{q=-\infty}^{\infty} \cdots\ k_l(\omega_{lmpq})\sin\epsilon_l(\omega_{lmpq}), \tag{43}$$

where the ellipsis denotes a function of the primary's radius and the secondary's orbital elements. The functions $k_l(\omega_{lmpq})$ are the dynamical analogs of the static Love numbers, while the phase lags corresponding to the tidal modes ω_{lmpq} are given by

$$\epsilon_l(\omega_{lmpq}) = \omega_{lmpq}\Delta t_l(|\omega_{lmpq}|) = |\,\omega_{lmpq}\,|\Delta t_l(|\omega_{lmpq}|)\mathrm{sgn}\,\omega_{lmpq} = \chi_{lmpq}\Delta t_l(\chi_{lmpq})\,\mathrm{sgn}\,\omega_{lmpq}. \tag{44}$$

Here the positively defined quantities

$$\chi_{lmpq} \equiv |\omega_{lmpq}| \tag{45}$$

are the forcing frequencies in the material, while the positively defined time lags Δt_{lmpq} are their functions.

Following Kaula (1964), the phase and time lags are often denoted with ϵ_{lmpq} and Δt_{lmpq}. For near-spherical bodies, though, the notations $\epsilon_l(\chi_{lmpq})$ and $\Delta t_l(\chi_{lmpq})$ would be preferable, because for such bodies the functional form of the dependency $\epsilon_{lmpq}(\chi)$ is defined by l s, but is ignorant of the values of the other three indices.[11] The same therefore applies to the time lag.

[10] When the role of the primary is played by a planet and the role of the perturbing secondary is played by the host star, the argument of the pericenter of the star as seen from the planet, ω, differs by π from the argument of the pericenter of the planet as seen from the star. Also note that in Equation (42) the letter ω with the subscript $lmpq$ denotes, as ever, a tidal mode, while the same letter without a subscript stands for the periapse. The latter use of this letter in Equation (42) is exceptional, in that elsewhere in the paper the letter ω, with or without a subscript, always denotes a tidal mode.

[11] Within the applicability realm of the elastic–viscoelastic analogy employed in Section 5.2 below, the functional form of the complex Love number $\bar{k}_l(\chi)$ of a near-spherical object is determined by index l solely, while the integers $m,\ p,\ q$ show up through the value of the frequency: $\bar{k}_l(\chi) = \bar{k}_l(\chi_{lmpq})$. This applies to the lag too, since the latter is related to $\bar{k}_l$ via Equation (62).

For triaxial bodies, the functional forms of the frequency dependencies of the Love numbers and phase lags do depend upon $m,\ p,\ q$ because of coupling between spherical harmonics. In those situations, notations $\bar{k}_{lmpq}$ and ϵ_{lmpq} become necessary (Dehant 1987a, 1987b; Smith 1974). The Love numbers of a slightly non-spherical primary differ from the Love numbers of the spherical reference body by a term of the order of the flattening, so a small non-sphericity can usually be ignored.

The forcing frequencies in the material of the primary, χ_{lmpq}, are positively defined. While the general formula for a Fourier expansion of a field includes integration (or summation) over both positive and negative frequencies, it is easy to demonstrate that in the case of real fields it is sufficient to expand over positive frequencies only. The condition of the field being real requires that the real part of a Fourier term at a negative frequency is equal to the real part of the term at an opposite, positive frequency. Hence, one can get rid of the terms with negative frequencies at the cost of doubling the appropriate terms with positive frequencies. (The convention is that the field is the real part of a complex expression.)

The tidal theory is a rare exception to this rule: here, a contribution of a Fourier mode into the potential is not completely equivalent to the contribution of the mode of an opposite sign. The reason for this is that the tidal theory is developed to render expressions for tidal forces and torques, and the sign of the tidal mode ω_{lmpq} shows up explicitly in those expressions. This happens because the phase lag in Equation (43) is the product (44) of the tidal mode ω_{lmpq} and the positively defined time lag Δt_{lmpq}.

This way, if we choose to expand tide over the positively defined frequencies χ only, we shall have to insert "by hand" the multipliers

$$\operatorname{sgn}\omega_{lmpq} = \operatorname{sgn}[(l-2p+q)\,n - m\,\dot{\theta}] \tag{46}$$

into the expressions for the tidal torque and force, a result to be employed below in formula (65). The topic is explained in greater detail in Efroimsky (2012).

5. COMPLEX LOVE NUMBERS AND THE ELASTIC–VISCOELASTIC ANALOGY

Let us recall briefly the switch from the stationary Love numbers to their dynamical counterparts, the Love operators. The method was probably pioneered by Zahn (1966) who applied it to a purely viscous planet. The method works likewise for an arbitrary linear rheological model insofar as the elastic–viscoelastic analogy (also referred to as the correspondence principle) remains in force.

5.1. From the Love Numbers to the Love Operators

A homogeneous near-spherical incompressible primary alters its shape and potential when influenced by a static point-like secondary. At a point $\vec{\boldsymbol{R}} = (R, \lambda, \phi)$, the potential due to a tide-generating secondary of mass $M^*_{\rm sec}$, located at $\vec{\boldsymbol{r}}^{\,*} = (r^*,\ \lambda^*,\ \phi^*)$ with $r^* \geqslant R$, can be expressed through the Legendre polynomials $P_l(\cos\gamma)$ or the Legendre functions $P_{lm}(\sin\phi)$:

$$\begin{aligned} W(\boldsymbol{R}\,,\ \boldsymbol{r}^{\,*}) &= \sum_{l=2}^{\infty} W_l(\boldsymbol{R}\,,\boldsymbol{r}^{\,*}) = -\frac{GM^*_{\rm sec}}{r^*}\sum_{l=2}^{\infty}\left(\frac{R}{r^*}\right)^l P_l(\cos\gamma) \\ &= -\frac{GM^*_{\rm sec}}{r^*}\sum_{l=2}^{\infty}\left(\frac{R}{r^*}\right)^l \sum_{m=0}^{l}\frac{(l-m)!}{(l+m)!}(2-\delta_{0m})P_{lm}(\sin\phi)P_{lm}(\sin\phi^*)\cos m(\lambda-\lambda^*), \end{aligned} \tag{47}$$

G being Newton's gravitational constant and γ being the angle between the vectors $\boldsymbol{r}^{\,*}$ and $\boldsymbol{R}$ originating from the primary's center. The latitudes $\phi,\ \phi^*$ are reckoned from the primary's equator, while the longitudes $\lambda,\ \lambda^*$ are reckoned from a fixed meridian on the primary.

The lth spherical harmonic $U_l(\boldsymbol{r})$ of the resulting change of the primary's potential at an exterior point $\boldsymbol{r}$ is connected to the lth spherical harmonic $W_l(\boldsymbol{R}\,,\ \boldsymbol{r}^{\,*})$ of the perturbing exterior potential via $U_l(\boldsymbol{r}) = (R/r)^{l+1}k_l\,W_l(\boldsymbol{R}\,,\ \boldsymbol{r}^{\,*})$, so the total change in the exterior potential of the primary becomes

$$U(\boldsymbol{r}) = \sum_{l=2}^{\infty} U_l(\boldsymbol{r}) = \sum_{l=2}^{\infty}\left(\frac{R}{r}\right)^{l+1} k_l\ W_l(\boldsymbol{R},\ \boldsymbol{r}^{\,*}). \tag{48}$$

While in Equation (47) $\boldsymbol{R}$ could lie either outside or on the surface of the primary, in Equation (48) it would be both convenient and conventional to make $\boldsymbol{R}$ a surface point. In both Equations (47) and (48), the vector $\boldsymbol{r}$ denotes an exterior point located above the surface point $\boldsymbol{R}$ at a radius $r \geqslant R$ (with the same latitude and longitude), while $\boldsymbol{r}^{\,*}$ signifies the position of the tide-raising secondary. The quantities k_l are the static Love numbers.

Under dynamical stressing, the Love numbers turn into operators:

$$U_l(\boldsymbol{r},\ t) = \left(\frac{R}{r}\right)^{l+1}\hat{k}_l(t)\ W_l(\boldsymbol{R},\ \boldsymbol{r}^{\,*},\ t'), \tag{49}$$

where integration over the semi-interval $t' \in [-\infty,\ t]$ is implied:

$$U_l(\boldsymbol{r},\ t) = \left(\frac{R}{r}\right)^{l+1}\int_{t'=-\infty}^{t'=t} k_l(t-t')\ \dot{W}_l\,(\boldsymbol{R},\ \boldsymbol{r}^{\,*},\ t')\,dt' \tag{50a}$$

$$= \left(\frac{R}{r}\right)^{l+1}[k_l(0)W(t) - k_l(\infty)W(-\infty)] + \left(\frac{R}{r}\right)^{l+1}\int_{-\infty}^{t}\dot{k}_l(t-t')\,W_l(\boldsymbol{R},\ \boldsymbol{r}^{\,*},\ t')\,dt'. \tag{50b}$$

Like in the compliance operator ((1) and (2)), here we also obtain the boundary terms: one corresponding to the instantaneous elastic reaction, $k_l(0)W(t)$, and another caused by the perturbation in the infinite past, $-k_l(\infty)W(-\infty)$. The latter term can be dropped by setting $W(-\infty)$ zero, while the former term may be included into the kernel in the same manner as in Equations (3)–(5):

$$\left(\frac{R}{r}\right)^{l+1} k_l(0)W(t) + \left(\frac{R}{r}\right)^{l+1} \int_{-\infty}^{t} \dot{k}_l(t-t')\, W_l(\boldsymbol{R},\ \boldsymbol{r}^*,\ t')\, dt' = \left(\frac{R}{r}\right)^{l+1} \int_{-\infty}^{t} \frac{d}{dt}[k_l(t-t') - k_l(0) + k_l(0)\Theta(t-t')]W_l(\boldsymbol{R}, \boldsymbol{r}^*, t')\, dt'. \tag{50c}$$

All in all, neglecting the unphysical term with $W(-\infty)$, and inserting the elastic term into the Love number, not as $k_l(0)$ but as $k_l(0)\,\Theta(t-t')$, we arrive at

$$U_l(\boldsymbol{r},\ t) = \left(\frac{R}{r}\right)^{l+1} \int_{-\infty}^{t} \dot{k}_l(t-t') W_l(\boldsymbol{R},\ \boldsymbol{r}^*,\ t')\, dt', \tag{51}$$

with $k_l(t-t')$ now incorporating the elastic reaction as $k_l(0)\,\Theta(t-t')$ instead of $k_l(0)$. For a perfectly elastic primary, the elastic reaction would be the only term present in the expression for $k_l(t-t')$. Then the time derivative of k_l would be $\dot{k}_l(t-t') = k_l\,\delta(t-t')$, with $k_l \equiv k_l(0)$ being the static Love number, and Equation (51) would reduce to $U_l(\boldsymbol{r},\ t) = (R/r)^{l+1} k_l\, W_l(\boldsymbol{R},\ \boldsymbol{r}^*,\ t)$, as in the static case.

Similar to Equation (11), the complex Love numbers are defined as the Fourier images of $\dot{k}_l\ (\tau)$:

$$\int_0^{\infty} \bar{k}_l(\chi) e^{i\chi\tau} d\chi = \dot{k}_l\ (\tau), \tag{52}$$

overdot denoting $d/d\tau$. Following Churkin (1998), the time derivatives $\dot{k}_l\ (t)$ can be called Love functions.[12] Inversion of Equation (52) renders:

$$\bar{k}_l(\chi) = \int_0^{\infty} \dot{k}_l(\tau)\ e^{-i\chi\tau}\, d\tau = k_l(0) + i\chi \int_0^{\infty} [\, k_l(\tau) - k_l(0)\,\Theta(\tau)\,]\ e^{-i\chi\tau}\, d\tau, \tag{53}$$

where integration from 0 is sufficient, as the future disturbance contributes nothing to the present distortion, wherefore $k_l(\tau)$ vanishes at $\tau < 0$. Recall that the time τ denotes the difference $t - t'$ and thus is reckoned from the present moment t backward into the past.

In the frequency domain, Equation (50) will take the shape of

$$\bar{U}_l(\chi) = \left(\frac{R}{r}\right)^{l+1} \bar{k}_l(\chi)\bar{W}_l(\chi), \tag{54}$$

with χ being the frequency, while $\bar{U}_l(\chi)$ and $\bar{W}_l(\chi)$ are the Fourier or Laplace components of the potentials $U_l(t)$ and $W_l(t)$. The frequency dependencies $\bar{k}_l(\chi)$ should be derived from the expression for $\bar{J}(\chi)$ or $\bar{\mu}(\chi) = 1/\bar{J}(\chi)$. These expressions follow from the rheological model of the medium.

Rigorously speaking, we ought to assume in expressions (52)–(54) that the spectral components are functions of the tidal mode ω and not of the forcing frequency χ. However, as explained in the end of Section 4, employment of the positively defined forcing frequencies is legitimate, insofar as we do not forget to attach the sign multipliers (46) to the terms of the Darwin–Kaula expansion for the tidal torque. Therefore, here and hereafter we shall expand over χ, with the said caveat kept in mind.

5.2. Complex Love Numbers as Functions of the Complex Compliance: The Elastic–Viscoelastic Analogy

The dependence of the static Love numbers on the static rigidity modulus $\mu(\infty)$ is

$$k_l^{(\text{static})} = \frac{3}{2\,(l-1)}\ \frac{1}{1 + A_l^{(\text{static})}}, \tag{55}$$

where

$$A_l^{(\text{static})} \equiv \frac{(2\,l^2 + 4\,l + 3)}{l\,g\,\rho\,R}\,\mu(\infty) = \frac{3\,(2\,l^2 + 4\,l + 3)}{4\,l\pi\,G\,\rho^2\,R^2}\,\mu(\infty) = \frac{3\,(2\,l^2 + 4\,l + 3)}{4\,l\pi\,G\,\rho^2\,R^2\,J(\infty)}, \tag{56}$$

with ρ, g, and R being the density, surface gravity, and radius of the body, and G being the Newton gravitational constant. The static rigidity modulus and its inverse, the static compliance, are denoted here with $\mu(\infty)$ and $J(\infty)$, respectively. These notations imply that we identify *static* with *relaxed*.

[12] Churkin (1998) used functions, which he denoted $k_l(t)$ and which were, due to a difference in notations, the same as our $\dot{k}_l\ (\tau)$.

Specifically, the static quadrupole Love number will read

$$k_2^{(\mathrm{static})} = \frac{3}{2}\ \frac{1}{1+A_2^{(\mathrm{static})}}, \tag{57}$$

where the quantity

$$A_2^{(\mathrm{static})} = \frac{57}{8\,\pi}\,\frac{\mu(\infty)}{G\,\rho^2\,R^2} \tag{58}$$

is sometimes referred to as $\tilde{\mu}$. Clearly, $A_2^{(\mathrm{static})}$ in Equation (57), as well as $A_l^{(\mathrm{static})}$ in Equation (55), is a dimensionless measure of strength-dominated versus gravity-dominated behavior.

It is not immediately clear whether the same expression also interconnects $\bar{k}_l(\chi)$ with $\bar{\mu}(\chi)$. Fortunately, though, a wonderful theorem called elastic–viscoelastic analogy, also known as the correspondence principle, ensures that the viscoelastic operational moduli $\bar{\mu}(\chi)$ or $\bar{J}(\chi)$ obey the same algebraic relations as the elastic parameters μ or J (see, e.g., Efroimsky 2012 and references therein). For this reason, the Fourier or Laplace images of the viscoelastic equation of motion[13] and of the constitutive equation look similar to their static counterparts, except that the stress, strain, and potentials are replaced with their Fourier or Laplace images, while k_l, μ, and J are replaced with the Fourier or Laplace images of $\dot{k}_l\ (t-t')$, $\dot{\mu}\ (t-t')$, and $\dot{J}\ (t-t')$. For example, the constitutive equation will look like $\bar{\sigma}_{\gamma\nu} = 2\bar{\mu}\bar{u}_{\gamma\nu}$. Therefore the solution to the problem will retain the mathematical form of $\bar{U}_l = \bar{k}_l\,\bar{W}_l$, with $\bar{k}_l$ keeping the same functional dependence on ρ, R, and $\bar{\mu}$ (or $\bar{J}$) as in Equation (56), except that now μ and J are equipped with overbars:

$$\bar{k}_l(\chi) = \frac{3}{2\,(l-1)}\ \frac{1}{1+A_l\ \bar{\mu}(\chi)/\mu} \tag{59a}$$

$$= \frac{3}{2\,(l-1)}\,\frac{1}{1+A_l\ J/\bar{J}(\chi)} = \frac{3}{2\,(l-1)}\,\frac{\bar{J}(\chi)}{\bar{J}(\chi)+A_l\ J}, \tag{59b}$$

where

$$A_l \equiv \frac{(2\,l^2+4\,l+3)\,\mu}{l\,g\,\rho\,R} = \frac{3\,(2\,l^2+4\,l+3)\,\mu}{4\,l\,\pi\,G\,\rho^2\,R^2} = \frac{3(2\,l^2+4\,l+3)\,J^{-1}}{4\,l\,\pi\,G\,\rho^2\,R^2}, \tag{60}$$

Although expression (60) for factors A_l is very similar to expression (56) for their static counterparts, an important difference between (56) and (60) should be pointed out. While in Equation (56) we had the static (relaxed) rigidity and compliance, $\mu(\infty)$ and $J(\infty) = 1/\mu(\infty)$, in Equation (60) the letters μ and J may stand for any benchmark values satisfying $J = 1/\mu$. This freedom stems from the fact that the products $A_l\ J$ entering Equation (59b) bear no dependence upon J or μ. The second term in the denominator of Equation (59a) contains $\bar{\mu}$. For convenience, we multiply and then divide $\bar{\mu}$ by some μ, and make the multiplier μ a part of A_l as in Equation (60). This makes it easier for us to compare (60) with its static predecessor (56). However, the constant μ in Equations (59) and (60) is essentially arbitrary and is not obliged to coincide with, say, the unrelaxed or relaxed rigidity. Accordingly, $J = 1/\mu$ is not obliged to be the unrelaxed or relaxed compliance.

The above caveat is important because in certain rheological models some of the unrelaxed or relaxed moduli may be zero or infinite. This will happen, for example, if we start with the Maxwell or Kelvin–Voigt body and perform a transition to a purely viscous medium. Fortunately, in realistic rheologies such things do not happen. Hence it will be convenient (and possible) to identify the J from Equation (60) with the *unrelaxed* compliance $J = J(0)$ emerging in the rheological model (33). Accordingly, the rigidity $\mu = 1/J$ from Equation (60) will be identified with the *unrelaxed* rigidity $\mu(0) = 1/J(0)$. This convention will play a crucial role down the road, when we derive formula (63).

Writing the lth complex Love number as

$$\bar{k}_l(\chi) = \mathcal{R}e[\bar{k}_l(\chi)] + i\,\mathcal{I}m[\bar{k}_l(\chi)] = |\bar{k}_l(\chi)|\ e^{-i\epsilon_l(\chi)}, \tag{61}$$

we express the phase lag $\epsilon_l(\chi)$ as

$$|\bar{k}_l(\chi)|\ \sin\epsilon_l(\chi) = -\,\mathcal{I}m[\bar{k}_l(\chi)]. \tag{62}$$

The importance of the products $|\bar{k}_l(\chi)|\ \sin\epsilon_l(\chi)$ lies in the fact that they show up in the terms of the Darwin–Kaula expansion of the tidal potential. As a result, it is these products, and not k_l/Q as some think, that emerge in the expansions for tidal forces and torques, and for the dissipation rate.

In an attempt to preserve the popular notation k_l/Q, one may *define* the inverse quality factor as the sine of the lag—see the discussion in Section 2.3. In this case, though, one would have to employ the tidal lag ϵ_l, and not the lag δ in the material (which we call the "seismic" lag). Accordingly, one will have to write not k_l/Q but k_l/Q_l where $1/Q_l \equiv \sin\epsilon_l$.

[13] In the equation of motion, we should neglect the acceleration term and the nonconservative inertial forces. Both omissions are justified at realistic frequencies (for details, see the Appendix to Efroimsky 2012).

Importantly, the functional form of the frequency dependence $\sin\epsilon_l(\chi)$ is different for different l. Thus an attempt to name $\sin\epsilon_l$ as $1/Q$ would give birth to a whole array of different functions $Q_l(\chi)$. For a triaxial body, things will become even more complicated—see footnote 11. To conclude, it is not advisable to denote $\sin\epsilon_l$ with $1/Q$.

It should be mentioned that the Darwin–Kaula theory of tides is equally applicable to tides in despinning and librating bodies. In all cases, the phase angle $\epsilon_l = \epsilon_l(\chi_{lmpq})$ parameterizes the lag of the appropriate component of the bulge, while the absolute value of the complex Love number $|\bar{k}_l| = |\,\bar{k}_l(\chi_{lmpq})\,|$ determines the magnitude of this component. The overall bulge being a superposition of these components, its height may vary in time.

5.3. The Tangent of the Tidal Lag

In the denominator of Equation (59a) the term 1 emerges due to self-gravitation, while $A_l\, J/\bar{J}(\chi) = A_l\,|\bar{\mu}(\chi)|/\mu$ describes how the bulk properties of the medium contribute to deformation and damping. So for a vanishing $A_l\, J/|\bar{J}(\chi)|$ we end up with the hydrostatic Love numbers $k_l = 3/(2\,(l-1))$, while the lag becomes nil, as will be seen shortly from Equation (64). On the contrary, for very large $A_l\, J/\bar{J}(\chi)$, we expect to obtain the Love numbers and lags ignorant of the shape of the body.

To see how this works out, combine formulae (35) and (59b), to arrive at

$$\tan\epsilon_l = -\frac{\mathcal{I}m[\bar{k}_l(\chi)]}{\mathcal{R}e[\bar{k}_l(\chi)]} = -\frac{A_l\, J\,\mathcal{I}m[\bar{J}(\chi)]}{\{\mathcal{R}e[\bar{J}(\chi)]\}^2 + \{\mathcal{I}m[\bar{J}(\chi)]\}^2 + A_l\, J\,\mathcal{R}e[\bar{J}(\chi)]} \tag{63a}$$

$$= \frac{A_l\left[\,\zeta\, z^{-1} + z^{-\alpha}\sin(\alpha\,\pi/2)\;\Gamma(1+\alpha)\,\right]}{\left[1 + z^{-\alpha}\cos(\alpha\pi/2)\;\Gamma(1+\alpha)\right]^2 + \left[\zeta\, z^{-1} + z^{-\alpha}\sin(\alpha\pi/2)\;\Gamma(1+\alpha)\right]^2 + A_l\,[1 + z^{-\alpha}\cos(\alpha\pi/2)\;\Gamma(1+\alpha)]}, \tag{63b}$$

with z being the dimensionless frequency defined by Equation (39).

Comparing this expression with expression (38) over different frequency bands, we shall be able to explore how the tidal lag ϵ_l relates to the lag in the material δ (the "seismic lag").

While expression (63b) is written for the Andrade model, the preceeding formula (63a) is general and works for an arbitrary linear rheology.

5.4. The Negative Imaginary Part of the Complex Love Number

As we already mentioned above, rheology influences the tidal behavior of a planet through the following sequence of steps. A rheological model postulates the form of $\bar{J}(\chi)$. This function, in its turn, determines the form of $\bar{k}_l(\chi)$, while the latter defines the frequency dependence of the products $|\bar{k}_l(\chi)|\sin\epsilon(\chi)$ which enter the tidal expansions.

To implement this concatenation, one has to express $|\bar{k}_l(\chi)|\sin\epsilon(\chi)$ via $\bar{J}(\chi)$. This can be done by combining Equation (59) with Equation (62). It renders

$$|\bar{k}_l(\chi)|\sin\epsilon_l(\chi) = -\mathcal{I}m[\bar{k}_l(\chi)] = \frac{3}{2\,(l-1)}\,\frac{-A_l\, J\,\mathcal{I}m[\bar{J}(\chi)]}{(\mathcal{R}e[\bar{J}(\chi)] + A_l\, J)^2 + (\mathcal{I}m[\bar{J}(\chi)])^2}, \tag{64}$$

a quantity often misnoted[14] as k_l/Q. Together, formulae (35) and (64) give us the frequency dependencies for the factors $|\bar{k}_l(\chi)|\sin\epsilon_l(\chi)$ entering the theory of bodily tides. For a detailed derivation of those dependencies, see Efroimsky (2012).

As explained in Section 4, employment of expressions (62)–(64) needs some care. Since both U and $\bar{k}_l$ are in fact functions not of the forcing frequency χ but of the tidal mode ω, formulae (62)–(64) should be equipped with multipliers $\mathrm{sgn}\,\omega_{lmpq}$, when plugged into the expression for the $lmpq$ component of the tidal torque. With this important caveat in mind, and with the subscripts $lmpq$ reinstalled, the complete expression will read:

$$|\bar{k}_l(\chi_{lmpq})|\sin\epsilon_l(\chi_{lmpq}) = \frac{3}{2\,(l-1)}\,\frac{-A_l\, J\,\mathcal{I}m[\bar{J}(\chi_{lmpq})]}{(\mathcal{R}e[\bar{J}(\chi_{lmpq})] + A_l\; J)^2 + (\mathcal{I}m[\bar{J}(\chi_{lmpq})])^2}\,\mathrm{sgn}\,\omega_{lmpq}, \tag{65}$$

a general formula valid for an arbitrary linear rheological model.

To make use of this and other formulae, it would be instructive to estimate the values of A_l for terrestrial objects of different size. In Table 1, we present estimates of A_2 for Iapetus, Mars, solid Earth, a hypothetical solid super-Earth having a density and rigidity of the solid Earth and a radius equal to 2 terrestrial radii ($R = 2\,R_\oplus$), and also a hypothetical super-Earth two times larger ($R = 4\,R_\oplus$) of the same rheology.

Taken the uncertainty of structure and the roughness of our estimate, all quantities in the table have been rounded to the first decimal. The values of Iapetus' and Mars' rigidity were borrowed from Castillo-Rogez et al. (2011) and Johnson et al. (2000), respectively.

In Figure 2, we compare the behavior of $k_2\,\sin\epsilon_2 = |\bar{k}_2(\chi)|\,\sin\epsilon_2(\chi)$ for the values of A_2 appropriate to Iapetus, Mars, solid Earth, and hypothetical super-Earths with $R = 2\,R_\oplus$ and $R = 4\,R_\oplus$, as given in Table 1. Self-gravitation pulls the tides down, mitigating their magnitude and the value of the tidal torque. Hence, the heavier the body, the lower the appropriate curve. This rule is observed well at low frequencies (the viscosity-dominated range). In the intermediate zone and in the high-frequency band (where anelasticity dominates friction), this rule starts working only for bodies larger than about twice Earth's size. If we fix the tidal frequency at a sufficiently high value, we shall see that the increase of the size from that of Iapetus to that of Mars and further to that of Earth results in an *increase* of the intensity of the tidal interaction. For an $R = 2\,R_\oplus$ super-Earth, the tidal factor $k_2\,\sin\epsilon_2$ is about the same as that for the solid Earth, and begins to decrease for larger radii (so the green curve for the larger super-Earth is located fully below the cyan curve for a smaller super-Earth).

[14] One can write the left-hand side of Equation (64) as k_l/Q only if the quality factor is defined through Equation (26) and endowed with the subscript l.

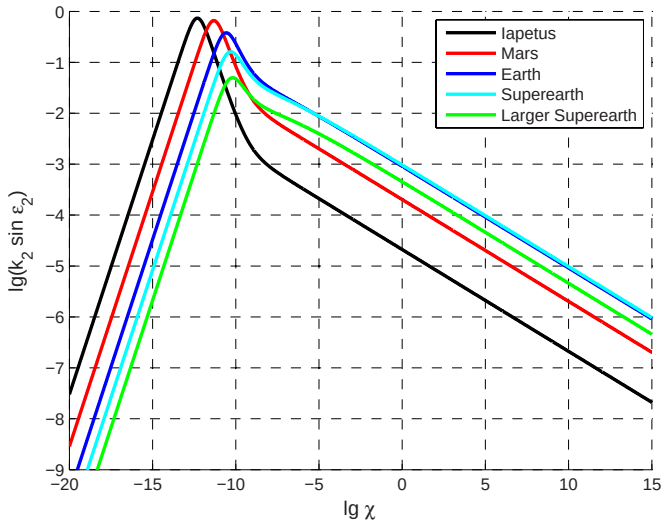

Figure 2. Negative imaginary part of the complex quadrupole Love number, $k_2 \sin\epsilon_2 = -\mathcal{I}m[\bar{k}_2(\chi)]$, as a function of the tidal frequency χ. The black, red, and blue curves refer, respectively, to Iapetus, Mars, and the solid Earth. The cyan and green curves refer to the two hypothetical superearths described in Table 1. These superearths have the same rheology as the solid Earth but have sizes $R = 2\,R_\oplus$ and $R = 4\,R_\oplus$. Each of these five objects is modeled with a homogeneous near-spherical self-gravitating Andrade body with $\alpha = 0.2$ and $\tau_A = \tau_M = 10^{10}$ s. In the limit of vanishing tidal frequency χ, the factors $k_2 \sin\epsilon_2$ approach zero, which is natural from the physical point of view. Indeed, an $lmpq$ term in the expansion for tidal torque contains the factor $k_l(\chi_{lmpq}) \sin\epsilon_l(\chi_{lmpq})$. On crossing the $lmpq$ resonance, where the frequency χ_{lmpq} goes through zero, the factor $k_l(\chi_{lmpq}) \sin\epsilon_l(\chi_{lmpq})$ must vanish, so that the $lmpq$ term of the torque could change its sign.

Table 1
Estimates of $A_2^{(\mathrm{static})}$ for Rigid Celestial Bodies

	Radius (R)	Mean Density (ρ)	Mean Relaxed Shear Rigidity ($\mu(\infty)$)	The Resulting Estimate for A_2
Iapetus	7.4×10^5 m	1.1×10^3 kg m^{-3}	4.0×10^9 Pa	200
Mars	3.4×10^6 m	3.9×10^3 kg m^{-3}	1.0×10^{11} Pa	19
Earth	6.4×10^6 m	5.5×10^3 kg m^{-3}	0.8×10^{11} Pa	2.2
A hypothetical super-Earth with $R = 2\,R_\oplus$ and the same rheology as Earth	4.5×10^8 m	5.5×10^3 kg m^{-3}	0.8×10^{11} Pa	0.55
A hypothetical super-Earth with $R = 4\,R_\oplus$ and the same rheology as Earth	9.0×10^8 m	5.5×10^3 kg m^{-3}	0.8×10^{11} Pa	0.14

Notes. The values of $A_2^{(\mathrm{static})}$ are calculated using Equation (58) and are rounded to the second figure.

6. TIDAL DISSIPATION VERSUS SEISMIC DISSIPATION IN THE ANELASTICITY-DOMINATED BAND

In this section, we shall address only the higher-frequency band of the spectrum, i.e., the range where anelasticity dominates viscoelasticity and the Andrade model is applicable safely. Mind though that the Andrade model can also embrace the near-Maxwell behavior, and thus can be applied to the low frequencies, provided we "tune" the dimensionless parameter ζ appropriately—see Section 3.4 above.

6.1. Response of a Sample of Material

At frequencies higher than some threshold value χ_0, dissipation in minerals is mainly due to anelasticity rather than to viscosity.[15] Hence, at these frequencies ζ should be of order unity or smaller, as can be seen from Equation (33b). This entails two consequences. First, the condition $\chi \gg 1/(\zeta\,\tau_M)$, i.e., $z \gg 1$ is obeyed reliably, for which reason the first term dominates the denominator in Equation (38). Second, either the condition $z \gg 1$ is stronger than $z \gg \zeta^{1/(1-\alpha)}$ or the two conditions are about equivalent. Hence the anelastic term dominates the numerator in Equation (38): $z^{-\alpha} \gg z^{-1}\,\zeta$.

Altogether, over the said frequency range, Equation (38) simplifies to:

$$\tan\delta \approx (\chi\,\tau_A)^{-\alpha} \sin\left(\frac{\alpha\,\pi}{2}\right) \Gamma(\alpha+1) = (\chi\,\zeta\,\tau_M)^{-\alpha} \sin\left(\frac{\alpha\,\pi}{2}\right) \Gamma(\alpha+1). \tag{66}$$

[15] For the solid Earth, this threshold is about 1 yr^{-1} (Karato & Spetzler 1990). Being temperature sensitive, the threshold may assume different values for other terrestrial planets. Also mind that the transition is not sharp and can extend over a decade or more.

Clearly, $\tan\delta \ll 1$, wherefore $\tan\delta \approx \sin\delta \approx \delta$. For the seismic quality factor, we then have:

$$^{(\text{seismic})}Q^{-1} \approx (\chi\ \tau_A)^{-\alpha} \sin\left(\frac{\alpha\,\pi}{2}\right) \Gamma(\alpha+1), \tag{67}$$

no matter which of the three definitions (21)–(23) we accept. Be mindful that here we use the term *seismic* broadly, applying it also to a sample in a lab.

6.2. Tidal Response of a Homogeneous Near-spherical Body

Recall that defect unpinning stays effective at frequencies above some threshold χ_0, which is likely to be above or, at least not much lower than, the inverse Maxwell time,[16] e.g., for the solid Earth, $\chi_0 \sim 1\ \text{yr}^{-1}$ while $\tau_M \sim 500$ yr. Over this frequency band, the free parameter ζ may be of order unity or slightly less than that. (This parameter grows as the frequencies become short of χ_0.) Under these circumstances, in Equation (63) we have: $\zeta z^{-1} \ll z^{-\alpha} \ll 1$, whence Equation (63) becomes

$$\tan\epsilon_l \approx \frac{A_l}{1+A_l} z^{-\alpha} \sin\left(\frac{\alpha\pi}{2}\right) \Gamma(1+\alpha). \tag{68}$$

In combination with Equation (66), this renders

$$\tan\epsilon_l = \frac{A_l}{1+A_l} \tan\delta. \tag{69}$$

Had we defined the quality factors as cotangents, like in Equation (23), then we would have to conclude from Equation (69) that the tidal and seismic quality factors coincide for small objects (with $A_l \gg 1$) and differ very considerably for super-Earths (i.e., for $A_l \ll 1$). Specifically, the so-defined quality factor Q_l of a super-Earth would be larger than its seismic counterpart Q by a factor of about A_l^{-1}.

In reality, the quality factors should be used for illustrative purposes only because practical calculations involve the factor $|\bar{k}_l(\chi_{lmpq})|\ \sin\epsilon_l(\chi_{lmpq})$ rendered by Equation (65). It is this factor which enters the $lmpq$ term of the Fourier expansion of tides. Insertion of Equations (36) and (37) into Equation (65) furnishes the following expression valid in the anelasticity-dominated band:

$$|\bar{k}_l(\chi_{lmpq})|\ \sin\epsilon_l(\chi_{lmpq}) \approx \frac{3}{2\,(l-1)}\ \frac{A_l}{(A_l+1)^2} \sin\left(\frac{\alpha\pi}{2}\right) \Gamma(\alpha+1)\,\zeta^{-\alpha}(\tau_M\,\chi_{lmpq})^{-\alpha}\ \text{sgn}\,\omega_{lmpq}, \quad \text{for} \quad \chi_{lmpq} \gg \chi_{\text{HI}}, \tag{70}$$

χ_{HI} being the boundary between the high and intermediate frequencies, i.e., between the anelasticity-dominated band and the transitional zone. Expression (70) resembles the frequency dependency for $|\bar{J}(\chi)|\ \sin\delta(\chi) = -\mathcal{I}m[\bar{J}(\chi)]$ at high frequencies (see Equation 36). In Figure 2, dependency (70) corresponds to the slowly descending slope on the far right.

A detailed derivation of Equation (70) from formulae (36)–(37) and (65) is presented in the Appendix to Efroimsky (2012). For terrestrial objects several times smaller than Earth (so $A_l \gg 1$), the threshold turns out to be

$$\chi_{\text{HI}} = \tau_M^{-1}\,\zeta^{\,\alpha/(1-\alpha)}. \tag{71}$$

For super-Earths (i.e., for $A_l \ll 1$), the threshold becomes

$$\chi_{\text{HI}} = \tau_A^{-1} = \tau_M^{-1}\,\zeta^{-1}. \tag{72}$$

Near the borderline between the anelasticity-dominated band and the transitional zone, the parameter ζ could be of order unity. It may as well be lower than unity, though not by much (hardly by an order of magnitude), because too low a value of ζ would exclude viscosity from the play completely. We, however, expect viscosity to be noticeable near the transitional zone.

Finally, it should be reiterated that at frequencies lower than some χ_0 the defect-unpinning process becomes less effective, so anelasticity becomes less effective than viscosity, and the free parameter ζ begins to grow. Hence, if the above estimates for χ_{HI} turn out to be lower than χ_0, we should set $\chi_{\text{HI}} = \chi_0$ "by hand."

7. TIDAL DISSIPATION VERSUS SEISMIC DISSIPATION IN THE VISCOSITY-DOMINATED BAND

When frequency χ becomes short of some χ_0, the rate of anelastic dissipation caused by defect unpinning decreases and viscosity begins to take over anelasticity.

If we simply assume the free parameter ζ to be of order unity everywhere, i.e., assume that the Maxwell and Andrade timescales are everywhere comparable, then application of the Andrade model will set χ_0 to be of order τ_M^{-1}. Anelasticity will dominate at frequencies above that threshold, while below it the role of viscosity will be higher. This approach, however, would be simplistic because the actual location of the threshold should be derived from microphysics and may turn out to differ noticeably from τ_M^{-1}. For

[16] Dislocations may break away from the pinning agents (impurities, nodes, or jogs), or the pinning agents themselves may move along with dislocations. These two processes are called "unpinning," and they go easier at low frequencies, as the energy barriers become lower (Karato & Spetzler 1990, Section 5.2.3).

example, in the terrestrial mantle the transition takes place at frequencies as high as 1 yr^{-1} (Karato & Spetzler 1990) and may be spread over a decade or more into lower frequencies, as we shall see from Equation (73).

Another somewhat simplistic option would be to assume that $\zeta \sim 1$ at frequencies above χ_0, and to set $\zeta = \infty$ at frequencies below χ_0. The latter would be equivalent to claiming that below this threshold the mantle is described by the Maxwell model. In reality, here we are just entering a transition zone, where ζ increases with the decrease of the frequency. While it is clear that in the denominator of Equation (38) the first term dominates, the situation with the numerator is less certain. Only after the condition

$$\zeta \gg (\chi\,\tau_M)^{(1-\alpha)/\alpha} \approx (\chi\,\tau_M)^4 \tag{73}$$

is obeyed, the viscous term $1/(\chi\,\tau_M)$ becomes leading. This way, although ζ begins to grow as the frequency decreases below χ_0, the frequency may need to decrease by another decade or more before threshold (73) is reached.

7.1. Response of a Sample of Material

Accepting the approximation that the transition zone is narrow[17] and that the predominantly viscous regime is already reached at χ_0 or shortly below, we approximate the tangent of the lag with

$$\tan\delta \approx (\chi\,\tau_M)^{-1}, \tag{74}$$

whence

$$\sin\delta \approx \begin{cases} (\chi\,\tau_M)^{-1} & \text{for} \quad \tau_M^{-1} \ll \chi \ll \chi_0, \\ 1 & \text{for} \quad 0 \leqslant \chi \ll \tau_M^{-1}. \end{cases} \tag{75}$$

7.2. Tidal Response of a Homogeneous Near-spherical Body

When viscosity dominates anelasticity, expression (63) gets reduced to the following form:

$$\tan\epsilon_l \approx \frac{A_l}{1 + A_l + (\zeta\,z^{-1})^2}\,\zeta\,z^{-1} = \frac{A_l}{1 + A_l + (\chi\,\tau_M)^{-2}}\,\frac{1}{\chi\,\tau_M}, \tag{76}$$

where comparison with Equation (74) renders

$$\tan\epsilon_l \approx \frac{A_l}{1 + A_l + (\chi\,\tau_M)^{-2}}\,\tan\delta = \frac{A_l}{1 + A_l + \tan^2\delta}\,\tan\delta. \tag{77}$$

Now two special cases should be considered separately.

7.2.1. Small Bodies and Small Terrestrial Planets

As illustrated by Table 1, small bodies and small terrestrial planets have $A_l \gg 1$. So formulae (76) and (77) take the form of

$$\tan\epsilon_l \approx \begin{cases} \dfrac{1}{\chi\,\tau_M} & \text{for} \quad \dfrac{1}{\tau_M\sqrt{A_l+1}} \ll \chi \ll \chi_0, \\ A_l\,\chi\,\tau_M & \text{for} \quad 0 \leqslant \chi \ll \dfrac{1}{\tau_M\sqrt{A_l+1}} \approx \dfrac{1}{\tau_M\sqrt{A_l}}, \end{cases} \tag{78}$$

and

$$\tan\epsilon_l \approx \begin{cases} \dfrac{A_l}{1+A_l}\tan\delta \approx \tan\delta & \text{for} \quad \dfrac{1}{\tau_M\sqrt{A_l+1}} \ll \chi \ll \chi_0, \\ \dfrac{A_l}{\tan\delta} & \text{for} \quad 0 \leqslant \chi \ll \dfrac{1}{\tau_M\sqrt{A_l+1}} \approx \dfrac{1}{\tau_M\sqrt{A_l}}. \end{cases} \tag{79}$$

Had we defined the quality factors as cotangents of ϵ_l and δ, we would be faced with a situation that may at first glance appear embarrassing: in the zero-frequency limit, the so-defined tidal Q_l would become *inversely* proportional to the so-defined seismic Q factor. This would, however, correspond well to an obvious physical fact: when the satellite crosses the $lmpq$ commensurability, the $lmpq$ term of the average tidal torque acting on a satellite must smoothly pass through nil, together with the $lmpq$ tidal mode. (For example, the orbital average of the principal tidal torque $lmpq = 2200$ must vanish when the satellite crosses the synchronous orbit.) For a more accurate explanation in terms of the $|\bar{k}_l(\chi)|\,\sin\epsilon_l(\chi)$ factors see Section 7.3 below.

[17] For a broader transition zone, the rheology will approach that of Maxwell at lower frequencies. This, though, will not influence our main conclusions.

7.2.2. Super-Earths

For super-Earths, we have $A_l \ll 1$, so Equation (77) becomes

$$\tan\epsilon_l \approx A_l\,\chi\,\tau_M = \frac{A_l}{\tan\delta} \quad \text{for} \quad 0 \leqslant \chi \ll \frac{1}{\tau_M\sqrt{A_l+1}} \approx \frac{1}{\tau_M}. \tag{80}$$

Here we encounter the same apparent paradox: had we defined the quality factors as cotangents of ϵ_l and δ, we would end up with a tidal Q_l inversely proportional to its seismic counterpart Q. A qualitative explanation to this "paradox" is the same as in the subsection above, a more accurate elucidation to be given shortly in Section 7.3.

Another seemingly strange feature is that in this case (i.e., for $A_l \ll 1$) the tangent of the tidal lag skips the range of inverse-frequency behavior and becomes linear in the frequency right below the inverse Maxwell time. This, however, should not surprise us because the physically meaningful products $k_l\,\sin\epsilon_l$ still retain a short range over which they demonstrate the inverse-frequency behavior. This can be understood from Figure 2. There, on each plot, a short segment to the right of the maximum corresponds to the situation when $k_l\,\sin\epsilon_l$ scales as inverse frequency—see formula (81) below.

Thus we once again see that the illustrative capacity of the quality factor is limited. To spare ourselves surprises and "paradoxes," we should always keep in mind that the actual calculations are based on the frequency dependence of $|\bar{k}_l(\chi_{lmpq})|\,\sin\epsilon_l(\chi_{lmpq})$.

7.3. Tidal Response in Terms of $|\bar{k}_l(\chi)|\sin\epsilon_l(\chi)$

Combining Equations (36) and (37) with Equation (65), one can demonstrate that in the intermediate-frequency zone the tidal factors scale as

$$|\bar{k}_l(\chi)|\,\sin\epsilon_l(\chi) \approx \frac{3}{2\,(l-1)}\,\frac{A_l}{(A_l+1)^2}\,(\tau_M\,\chi)^{-1}, \quad \text{for} \quad \tau_M^{-1} \gg \chi \gg \tau_M^{-1}\,(A_l+1)^{-1}, \tag{81}$$

which corresponds to the short segment on the right of the maximum on Figure 2.

From the same formulae (36)–(37) and (65), it ensues that the low-frequency behavior is

$$|\bar{k}_l(\chi)|\,\sin\epsilon_l(\chi) \;\approx\; \frac{3}{2\,(l-1)}A_l\,\tau_M\,\chi, \quad \text{for} \quad \tau_M^{-1}\,(A_l+1)^{-1} \gg \chi, \tag{82}$$

a regime illustrated by the slope located on the left of the maximum on Figure 2.

Details of the derivation of Equations (81) and (82) can be found in the Appendix to Efroimsky (2012).

Just as expression (70) resembled the frequency dependency (36) for $|\bar{J}(\chi)|\,\sin\delta(\chi)$ at high frequencies, so Equation (81) resembles the behavior of $|\bar{J}(\chi)|\,\sin\delta(\chi)$ at low frequencies. At the same time, Equation (82) demonstrates a feature inherent only in tides, and not in the behavior of a sample of material: at $\chi < \tau_M^{-1}(A_l+1)^{-1} = (\mu/\eta)\times(A_l+1)^{-1}$, the factor $|\bar{k}_l(\chi)|\,\sin\epsilon_l(\chi)$ becomes linear in χ. This is not surprising, as the $lmpq$ component of the average tidal torque or force must pass smoothly through zero and change its sign when the $lmpq$ commensurability is crossed (and the $lmpq$ tidal mode goes through zero and changes sign).

8. WHY THE $lmpq$ COMPONENT OF THE TIDAL TORQUE DOES NOT SCALE AS R^{2l+1}

A Fourier component $\mathcal{T}_{lmpq}$ of the tidal torque acting on a perturbed primary is proportional to $R^{2l+1}\,k_l\,\sin\epsilon_l$, where R is the primary's mean equatorial radius. Neglect of the R-dependence of the tidal factors $k_l\,\sin\epsilon_l$ has long been a source of misunderstanding of how the torque scales with the radius.

From formulae (70) and (81), we see that everywhere except in the closest vicinity of the resonance the tidal factors are proportional to $A_l/(1+A_l)^2$ where $A_l \sim R^{-2}$ according to Equation (60). Hence the overall dependence of the tidal torque upon the radius becomes:

Over the frequency band $\chi \gg \tau_M^{-1}\,(1+A_l)^{-1}$,

$$\mathcal{T}_{lmpq} \;\sim\; R^{2l+1}k_l\,\sin\epsilon_l \sim [(R^{2l+1}\,A_l)/(1+A_l)^2] \sim \begin{cases} R^{2l-1}, & \text{for} \quad A_l \ll 1 \text{ (super-Earths)},\\ R^{2l+3}, & \text{for} \quad A_l \gg 1 \text{ (small bodies, small terrestrial planets)}. \end{cases} \tag{83}$$

In the closest vicinity of the $lmpq$ commensurability, i.e., when the tidal frequency χ_{lmpq} approaches zero, the tidal factors behavior is described by Equation (82). This furnishes a different scaling law for the torque, and the form of this law is the same for telluric bodies of all sizes:

Over the frequency band $\chi \;\ll\; \tau_M^{-1}\,(1+A_l)^{-1}$,

$$\mathcal{T}_{lmpq} \sim R^{2l+1}k_l\,\sin\epsilon_l \sim R^{2l+1}\,A_l \sim\; R^{2l-1}. \tag{84}$$

9. CONCLUSIONS AND EXAMPLES

Within the anelasticity-dominated band, the phase lags in a homogeneous near-spherical body and in a sample of material interrelate as

$$\tan\epsilon_l \;=\; (A_l/1+A_l)(\tan\delta) \approx \begin{cases} A_l\tan\delta & \text{for} \quad A_l \ll 1 \text{ (super-Earths)},\\ \tan\delta & \text{for} \quad A_l \gg 1 \text{ (small bodies, small terrestrial planets)}. \end{cases} \tag{85}$$

However, within the transitional zone, the link between the seismic and tidal dissipation rates becomes more complicated.

The interrelation between the tidal and seismic damping becomes apparently paradoxical at low frequencies, where viscosity dominates. As can be seen from Equations (78)–(80), in the zero-frequency limit the tidal and seismic Qs (if defined as cotangents of the appropriate lags) become *inversely* proportional to one another:

$$\tan\epsilon_l \;\approx A_l\,\chi\,\tau_M = \frac{A_l}{\tan\delta} \quad \text{for} \quad 0 \leqslant \chi \ll \frac{1}{\tau_M\sqrt{A_l+1}}. \tag{86}$$

This behavior, however, has a good qualitative explanation—the average tidal torque $lmpq$ should vanish on crossing of the $lmpq$ resonance.

While in qualitative discussions it is easier to deal with the quality factors Q_l, in practical calculations we should rely on the factors $k_l\,\sin\epsilon_l$, which show up in the Darwin–Kaula expansion of tides. Just as $\tan\epsilon_l$, so the quantity $k_l\,\sin\epsilon_l$ too becomes linear in χ for low values of χ. As we saw in Section 7.3, this happens over frequencies below $\chi \ll 1/(\tau_M(A_l+1))$. The slight difference between this threshold and the one shown in Equation (86) stems from the fact that not only the lag but also the Love number is frequency dependent.

The factors $k_l\,\sin\epsilon_l$ bear dependence upon the radius R of a tidally disturbed primary, and the form of this dependence is not always trivial. At low frequencies, this dependence follows the intuitively obvious rule that the heavier the body the stronger it mitigates tides (and thence the smaller the value of $k_l\,\sin\epsilon_l$). However, at high frequencies the calculated frequency dependence obeys this rule only beginning from sizes about double or larger than the size of the Earth, i.e., when self-gravitation clearly plays a larger role in tidal friction than the rheology does—see the discussion at the end of Section 5.4.

The dependence of $k_l\,\sin\epsilon_l$ upon R helps one to write down the overall R-dependence of the tidal torque. Contrary to the common belief, the $lmpq$ component of the torque does *not* scale as R^{2l+1}; see formulae (83) and (84).

Here follow some examples illustrating how our machinery applies to various celestial bodies.

1. For small bodies and small terrestrial planets, the effect of self-gravitation is negligible, except in the closest vicinity of the zero frequency. Accordingly, for these bodies there is no difference between the tidal and seismic dissipations.[18]
   Things change in the closest vicinity of the zero frequency. As can be observed from the second line of Equation (78), for small bodies and small planets the tangent of the tidal lag becomes linear in the tidal frequency χ when the frequency χ becomes short of a certain threshold:[19] $\chi \ll 1/(\tau_M\sqrt{A_l+1}) \approx 1/(\tau_M\sqrt{A_l})$. As can be seen from Equation (82), the tidal factor $k_l\,\sin\epsilon_l \equiv |\bar{k}_l(\chi)|\,\sin\epsilon_l(\chi)$ becomes linear in χ for $\chi \ll \tau_M^{-1}\,(A_l+1)^{-1} \approx \tau_M^{-1}\,A_l^{-1}$.
2. Tidal dissipation in super-Earths is much less efficient than in smaller terrestrial planets or moons—a circumstance that should reduce considerably the rates of orbit circularization. This cautionary point has ramifications also upon the other tidal-dynamic timescales (e.g., despinning, migration).
   In simple words, self-gravity reduces tidal dissipation because gravitational attraction pulls the tidal bulge back down, and thus reduces strain in a way similar to material strength.
   As can be seen from Equation (80), at tidal frequencies χ lower than the inverse Maxwell time,[20] the tangent of the tidal lag changes its behavior considerably, thereby avoiding divergence at the zero frequency. According to Equation (82), the same pertains to the factor $k_l\,\sin\epsilon_l$.
3. While the role of self-gravity is negligible for small planets and is dominant for super-Earths, the case of Earth is intermediate. For our mother planet, the contribution of self-gravitation into the Love numbers and phase lags is noticeable, though probably not leading. Indeed, for $\mu \approx 0.8\times10^{11}$ Pa, one arrives at:

$$A_2 \;\approx 2.2, \tag{87}$$

   so formula (69) tells us that Earth's tidal quality factor is a bit larger than its seismic counterpart, *taken at the same frequency*:[21]

$$^{(\text{tidal})}Q_2^{(\text{solid Earth})} \approx 1.5\times\,{}^{(\text{seismic})}Q^{(\text{solid Earth})}. \tag{88}$$

   The geodetic measurements of semidiurnal tides, carried out by Ray et al. (2001), yield $^{(\text{tidal})}Q_2^{(\text{solid Earth})} \approx 280$. The seismic quality factor $^{(\text{seismic})}Q^{(\text{solid Earth})}$ varies over the mantle, assuming values from 100 through 300. Accepting 200 for an arguable average, we see that Equation (88) furnishes a satisfactory qualitative estimate.

[18] This can be understood also through the following line of reasoning. For small objects, we have $A_l \gg 1$; so the complex Love numbers (59b) may be approximated with

$$\bar{k}_l(\chi) = -\frac{3}{2}\,\frac{\bar{J}\,(\chi)}{\bar{J}\,(\chi)+A_l\,J} = -\frac{3}{2}\,\frac{\bar{J}\,(\chi)}{A_l\,J} + O(|\bar{J}/(A_l\,J)|^2).$$

The latter entails

$$\tan\epsilon_l(\chi) \;\equiv -\frac{\mathcal{I}m[\bar{k}_l(\chi)]}{\mathcal{R}e[\bar{k}_l(\chi)]} \;\approx -\frac{\mathcal{I}m[\bar{J}(\chi)]}{\mathcal{R}e[\bar{J}(\chi)]} = \tan\delta(\chi),$$

which is, in fact, correct *up to a sign*—see the closing paragraph of Section 5.1.

[19] Recall that for small objects $A_l \gg 1$.

[20] For super-Earths, $A_l \ll 1$.

[21] When Benjamin et al. (2006) say that, according to their data, the tidal quality factor is slightly lower than the seismic one, these authors compare the two Q factors measured at different frequencies. Hence their statement does not contradict our conclusions.

This close hit should not of course be accepted too literally, taken Earth's complex structure and the uncertainty in our knowledge of Earth's rigidity. Still, on a qualitative level, we may enjoy this proximity with cautious optimism.

4. The case of the Moon deserves a special attention. Fitting of the LLR data to the power scaling law $Q \sim \chi^p$ has rendered a small *negative* value of the exponential: $p = -0.19$ (Williams et al. 2001). Further attempts by the JPL team to reprocess the data have led to $p = -0.07$. According to Williams & Boggs (2008, pp. 110–111), "There is a weak dependence of tidal specific dissipation Q on period. The Q increases from ∼30 at a month to ∼35 at one year. Q for rock is expected to have a weak dependence on tidal period, but it is expected to decrease with period rather than increase. The frequency dependence of Q deserves further attention and should be improved."

   To understand the origin of the small negative value of the power, recall that it emerged through fitting of the tidal Q_2 and not of the seismic Q. If future laser ranging confirms these data, this will mean that the principal tide in the Moon is located close to the maximum of the inverse tidal quality factor, i.e., close to the maximum taken by $\tan\epsilon_2$ in Equation (78) at the frequency inverse to $\tau_M \sqrt{A_l}$. Rigorously speaking, it was of course the factor $k_2 \sin\epsilon_2$ which was actually observed. The maximum of this factor is attained at the frequency $\tau_M^{-1} (A_l + 1)^{-1}$, as can be seen from Equations (81) to (82). It then follows from the LLR data that the corresponding timescale $\tau_M (A_l + 1)$ should be of order 0.1 year. As explained in Efroimsky (2012), this would set the mean viscosity of the Moon as low as

$$\eta_{\rm Moon} = 3 \times 10^{16}\ {\rm Pa\ s}, \tag{89}$$

   which in its turn would imply a very high concentration of the partial melt in the low mantle—quite in accordance with the existing models (Nakamura et al. 1974; Weber et al. 2011).

   The future LLR programs may be instrumental in resolving this difficult issue. The value of the exponential p will have ramifications for the current models of the lunar mantle.

10. COMPARISON OF OUR RESULT WITH THAT OF GOLDREICH (1963)

A formula coinciding with our Equation (69) was obtained, through remarkably economic and elegant semi-qualitative reasoning, by Peter Goldreich (1963).

The starting point in that paper was the observation that the peak work performed by the second-harmonic disturbing potential should be proportional to this potential taken at the primary's surface, multiplied by the maximal surface inequality:

$$E_{\rm peak} \sim R^5 \frac{R}{1 + 19\,\mu/(2\,g\,\rho\,R)} \sim \frac{R^7}{19\,\mu + 2\,g\,\rho\,R}\ , \tag{90}$$

R being the primary's radius.

In the static theory of Love, the surface strain is proportional to $R^2/(19\,\mu + 2\,g\,\rho\,R)$. The energy loss over a cycle must be proportional to the square of the surface strain. Integration over the volume will give an extra multiplier of R^3, up to a numerical factor:

$$\Delta E_{\rm cycle} \sim -\frac{R^7}{(19\,\mu + 2\,g\,\rho\,R)^2}. \tag{91}$$

Comparison of Equations (90) and (91) rendered

$$Q = -\frac{2\pi\,E_{\rm peak}}{\Delta E_{\rm cycle}} \sim (19\,\mu + 2\,g\,\rho\,R)\,,$$

wherefrom Goldreich (1963) deduced that

$$\frac{Q}{Q_0} = 1 + \frac{2\,g\,\rho\,R}{19\,\mu},$$

Q_0 being the value of Q for a body where self-gravitation is negligible. This coincides with our formula (69).

In reality, the coincidence of our results is only partial for two reasons.

1. First, our derivation of the right-hand side of (63) was based on the prior convention that the quantity J entering expression (60) is the *unrelaxed* compliance $J(0)$ of the mantle. Accordingly, the quantity $\mu = 1/J$ entering the expression for A_l should be the *unrelaxed* rigidity $\mu(0) = 1/J(0)$. In Goldreich (1963), however, the static, i.e., *relaxed*, moduli were implied.

   In Goldreich (1963), this mismatch was tolerable because the paper was devoted to small bodies. For these objects, A_l is large, no matter whether we plug the relaxed or unrelaxed μ into Equation (56). Thence the difference between the tidal and seismic Q factors is small, as can be seen from the second line of Equation (85).

   For Earths and super-Earths, however, the distinction between the unrelaxed and relaxed (static) moduli is critical. As can be seen from the first line of Equation (85), the tidal Q factor is inversely proportional to A_l and, thereby, is inversely proportional to the mantle rigidity μ. As well known (e.g., Ricard et al. 2009, Figure 3), the unrelaxed μ of the mantle exceeds the relaxed μ by about two orders of magnitude.

2. Second, as our calculation demonstrates, the simple interrelation given by Equations (69) and (85) works *only in the anelasticity-dominated band*. In the transition zone (which begins, in the solid Earth, at timescales longer than ∼1 yr) and in the viscosity-dominated band of lower frequencies, the interrelation between the tidal and seismic lagging is more complicated, and it deviates from Goldreich's formula in a fundamental way. In the zero-frequency limit the cleavage between the tidal and seismic dissipation laws gets especially large: the tidal and seismic Qs become not proportional but *inversely* proportional to one another. Description of tidal lagging in all these low-frequency bands requires a rheological model and the subsequent mathematics, and cannot be obtained through the simple arguments used by Goldreich (1963).

Despite these differences, the estimate by Goldreich (1963) provided as close a hit as was possible without resorting to heavy mathematics. The elegance of Peter Goldreich's arguments and the depth of his insight are especially impressive, taken the complexity of the problem and the volume of calculations required to obtain the exact answer.

To a large extent, my understanding of the theory of bodily tides was developed through the enlightening conversations which I had on numerous occasions with Bruce Bills, Julie Castillo-Rogez, Véronique Dehant, Sylvio Ferraz-Mello, Valéry Lainey, Valeri Makarov, Francis Nimmo, Stan Peale, Tim Van Hoolst, and James G. Williams. It is a great pleasure for me to thank deeply all these colleagues for their time and advice. Needless to say, none of them shares the responsibility for my possible omissions.

I also wish to pay tribute to the late Vladimir Churkin, whose tragic death prevented him from publishing his preprint cited in this paper. Written with a great pedagogical mastership, the preprint helped me to understand how the Love-number formalism should be combined with rheology.

My special gratitude is due to Shun-ichiro Karato for the help he so kindly provided to me when I was just opening for myself this intriguing area, and for the stimulating exchanges which we have had for years since then.

Last, and by no means least, I sincerely appreciate the support from my colleagues at the U.S. Naval Observatory, especially John Bangert.

APPENDIX

Table 2
Symbol Key

Symbol	Definition
A_l	Dimensionless product emerging in the denominator of the expression for the Love number k_l
E	Energy
$\mathcal{E}$	Empirical constant having the dimensions of time, in the generic rheological law (27)
g	Surface gravity
G	Newton's gravitational constant
l	Degree (spherical harmonics, Legendre polynomials)
m	Order (spherical harmonics, associated Legendre polynomials)
J, $J(0)$	Unrelaxed compliance
$J(\infty)$	Relaxed compliance
$J(t-t')$	Creep-response function (compliance function, kernel of the compliance operator)
$\hat{J}$	Compliance operator
k_l	Tidal Love number of degree l
$k_l(t-t')$	Kernel of the Love operator of degree l
$\hat{k}_l$	Love operator of degree l
$\bar{k}_l(\chi)$	Fourier component, at frequency χ, of the time derivative of the kernel $k_l(t-t')$
$\mathcal{M}$	Mean anomaly
n	Mean motion
p	Exponential in the generic rheological law (27)
P_l	Legendre polynomials of degree l
P_{lm}	Legendre associated functions (associated Legendre polynomials) of degree l and order m
Q	Dissipation quality factor
r	Distance
$\boldsymbol{r}$	Vector connecting the center of the tidally perturbed body (interpreted as the primary) with a point exterior to this body
$\boldsymbol{r}^*$	Vector connecting the center of the tidally perturbed body (the primary) with a point-like tide-raising secondary
R	Primary's mean radius
t	Time
$u_{\gamma\nu}$	Shear strain tensor
$\bar{u}_{\gamma\nu}(\chi)$	Fourier component, at frequency χ, of the shear strain tensor
U	Change in the potential of the tidally perturbed body (interpreted as the primary)
W	Disturbing potential generated by the tide-raising body (interpreted as the secondary)
α, β	Parameters of the Andrade model
γ, ν	Tensor indices
Γ	Gamma function
δ	Material phase lag
Δt	Time lag
ϵ	Tidal phase lag

Table 2
(Continued)

Symbol	Definition
ϵ_{lmpq}	Tidal phase lag of the mode $lmpq$ in the Darwin–Kaula expansion
λ	Longitude
ζ	Parameter of the reformulated Andrade model (ratio of the anelastic timescale τ_A to the Maxwell time τ_M)
η	Viscosity
μ, $\mu(0)$	Unrelaxed shear modulus (unrelaxed rigidity)
$\mu(\infty)$	Relaxed shear modulus (relaxed rigidity)
$\mu(t-t')$	Stress-relaxation function (kernel of the rigidity operator)
$\hat{\mu}$	Rigidity operator
ϕ	Latitude
ρ	Mass density
$\sigma_{\gamma\nu}$	Shear stress tensor
$\bar{\sigma}_{\gamma\nu}(\chi)$	Fourier component, at frequency χ, of the shear stress tensor
τ	Time
τ_M	Maxwell time (viscoelastic timescale)
τ_A	Andrade time (anelastic timescale)
$\mathcal{T}$	Tidal torque
$\Theta(t-t')$	Heaviside function
θ	Sidereal angle of the tidally disturbed body (interpreted as the primary)
$\dot{\theta}$	Spin rate of the primary
φ_σ , φ_u	Initial phases of the stress and strain
χ	Frequency
χ_0	Frequency threshold marking the boundary between the anelasticity- and viscosity-dominated frequency bands
χ_{lmpq}	Physical frequencies of deformation emerging in the tidal theory (absolute values of the tidal modes $\omega_{\rm lmpq}$)
ω_{lmpq}	Tidal modes in the Darwin–Kaula expansion of tides
ω	Argument of the pericenter
Ω	Longitude of the node

REFERENCES

Andrade, E. N. da C. 1910, Proc. Royal Society of London, Series A, 84, 1
Benjamin, D., Wahr, J., Ray, R. D., Egbert, G. D., & Desai, S. D. 2006, Geophys. J. Int., 165, 3
Birger, B. I. 2007, Izv. Phys. Solid Earth, 49, 635
Carter, J. A., Winn, J. N., Holman, M. J., et al. 2011, ApJ, 730, 82
Castillo-Rogez, J. 2009, AAS, DPS meeting 41, Abstract 61.07
Castillo-Rogez, J. C., Efroimsky, M., & Lainey, V. 2011, J. Geophys. Res.—Planets, 116, E09008
Churkin, V. A. 1998, The Love Numbers for the Models of Inelastic Earth, Preprint No. 121 (in Russian; St. Petersburg: Institute of Applied Astronomy)
Cottrell, A. H., & Aytekin, V. 1947, Nature, 160, 328
Dehant, V. 1987a, Phys. Earth Planet. Inter., 49, 97
Dehant, V. 1987b, Phys. Earth Planet. Inter., 49, 242
Duval, P. 1978, J. Glaciol., 21, 621
Eanes, R. J. 1995, PhD thesis, Univ. Texas at Austin
Eanes, R. J., & Bettadpur, S. V. 1996, in IAG Symp. Ser. 116, Global Gravity Field and Its Variations, ed. R. H. Rapp, A. A. Cazenave, & R. S. Nerem (New York: Springer), 30
Efroimsky, M. 2012, Celest. Mech. Dyn. Astron., in press (arXiv:1105.6086)
Efroimsky, M., & Lainey, V. 2007, J. Geophys. Res.—Planets, 112, E12003
Efroimsky, M., & Williams, J. G. 2009, Celest. Mech. Dyn. Astron., 104, 257
Findley, W. N., Lai, J. S., & Onaran, K. 1976, Creep and Relaxation of Nonlinear Viscoelastic Materials (New York: Dover), 384
Fontaine, F. R., Ildefonse, B., & Bagdassarov, N. 2005, Geophys. J. Int., 163, 1025
Goldreich, P. 1963, MNRAS, 126, 257
Gribb, T. T., & Cooper, R. F. 1998, J. Geophys. Res.—Solid Earth, 103, B27267
Henning, W. G., O'Connell, R., & Sasselov, D. 2009, ApJ, 707, 1000
Johnson, C. L., Solomon, S. C., Head, J. W., et al. 2000, Icarus, 144, 313
Karato, S.-i. 2008, Deformation of Earth Materials. An Introduction to the Rheology of Solid Earth (Cambridge: Cambridge Univ. Press)
Karato, S.-i., & Spetzler, H. A. 1990, Rev. Geophys., 28, 399
Kaula, W. M. 1964, Rev. Geophys., 2, 661
Léger, A., Rouan, D., Schneider, J., et al. 2009, A&A, 506, 287
McCarthy, C., Goldsby, D. L., & Cooper, R. F. 2007, in 38th Lunar and Planetary Science Conf. Ser. XXXVIII, Transient and Steady-State Creep Responses of Ice-I/Magnesium Sulfate Hydrate Eutectic Aggregates, 2007 March 12–16, League City, TX (LPI Contribution No 1338), 2429, http://www.lpi.usra.edu/meetings/lpsc2007/pdf/2429.pdf
Mitchell, B. 1995, Rev. Geophys., 33, 441
Nakamura, Y., Latham, G., Lammlein, D., et al. 1974, Geophys. Res. Lett., 1, 137
Nimmo, F. 2008, Paper presented at the Science of Solar System Ices Workshop, Tidal Dissipation and Faulting (Oxnard, CA: Lunar and Planetary Institute), http://www.lpi.usra.edu/meetings/scssi2008/pdf/9007.pdf
Ray, R. D., Eanes, R. J., & Lemoine, F. G. 2001, Geophys. J. Int., 144, 471
Ricard, Y., Matas, J., & Chambat, F. 2009, Phys. Earth Planet. Inter., 176, 124
Shito, A., Karato, S.-I., & Park, J. 2004, Geophys. Res. Lett., 31, L12603
Smith, M. 1974, Geophys. J. R. Astron. Soc., 37, 491
Stachnik, J. C., Abers, G. A., & Christensen, D. H. 2004, J. Geophys. Res.—Solid Earth, 109, B10304
Tan, B. H., Jackson, I., & Fitz Gerald, J. D. 1997, Geophys. Res. Lett., 24, 1055
Tyler, R. H. 2009, Geophys. Res. Lett., 36, L15205
Weber, R. C., Lin, P.-Y., Garnero, E., Williams, Q., & Lognonné, P. 2011, Science, 331, 309
Weertman, J., & Weertman, J. R. 1975, Annu. Rev. Earth Planet. Sci., 3, 293
Williams, J. G., & Boggs, D. H. 2008, in Proc. 16th International Workshop on Laser Ranging, Lunar Core and Mantle, What Does LLR See?, ed. S. Schilliak (Warsaw: Space Research Centre, Polish Academy of Sciences), 101, p. 110–111 http://cddis.gsfc.nasa.gov/lw16/docs/papers/sci_1_Williams_p.pdf, http://cddis.gsfc.nasa.gov/lw16/docs/papers/proceedings_vol2.pdf
Williams, J. G., Boggs, D. H., Yoder, C. F., Ratcliff, J. T., & Dickey, J. O. 2001, J. Geophys. Res.—Planets, 106, 27933
Zahn, J.-P. 1966, Ann. Astrophys., 29, 313
Zharkov, V. N., & Gudkova, T. V. 2009, Planet. Space Sci., 57, 288